MODULATION OF PHOSPHORESCENCE BY MICROWAVES

J. SCHMIDT

MODULATION OF PHOSPHERESCENCE BY MICROWAVES

MODULATION OF PHOSPHORESCENCE BY MICROWAVES

PROEFSCHRIFT

TER VERKRIJGING VAN DE GRAAD VAN DOCTOR IN
DE WISKUNDE EN NATUURWETENSCHAPPEN AAN
DE RIJKSUNIVERSITEIT TE LEIDEN, OP GEZAG VAN
DE RECTOR MAGNIFICUS DR. C. SOETEMAN,
HOOGLERAAR IN DE FACULTEIT DER LETTEREN,
TEN OVERSTAAN VAN EEN COMMISSIE UIT DE SENAAT
TE VERDEDIGEN OP WOENSDAG 2 JUNI 1971
TE KLOKKE 15.15 UUR

DOOR

JAN SCHMIDT

GEBOREN TE AMSTERDAM IN 1937

1971
BRONDER-OFFSET N.V.
ROTTERDAM

Promotor: Prof. Dr. J.H. van der WAALS

S T E L L I N G E N

1. Het experiment beschreven in hoofdstuk 6 van dit proefschrift is verwant aan het coherentie experiment van Chase aan de Γ_8-aangeslagen toestand van Eu^{2+} in CaF_2. Het essentiële verschil is dat hij de interferentie waarneemt in het uitgezonden licht zoals die bepaald wordt door de niet-diagonale elementen uit de dichtheidsmatrix.

   Chase, L.L., 1968, Phys.Rev.Letters, 21, 888.

2. Van Santen stelt, dat een relaxatie die leidt tot Boltzmann evenwicht tussen twee stralende niveaus de faserelatie tussen de twee toestanden zodanig beïnvloedt, dat geen zwevingen in de straling kunnen worden waargenomen. In werkelijkheid kunnen zwevingen ook dan nog optreden.

   Van Santen, R.A., 1971, On the theory of resonant scattering, Proefschrift Leiden, p. 67.

3. Maier, Haeberlen en Wolf hebben aangetoond, dat de spin-rooster relaxatietijd T_1 van de protonen in een anthraceen éénkristal wordt verkort door de aanwezigheid van triplet excitonen. In analogie hiermee zou men verwachten dat ook gelocaliseerde triplettoestanden een verkorting van T_1 bewerkstelligen. Het is theoretisch aan te tonen dat dit effect in het laatste geval waarschijnlijk te klein is om te worden waargenomen.

   Maier, G., Haeberlen, U. en Wolf, H.C., 1967, Phys.Letters 25A, 323.

4. Charlton en Bargon stellen selectieregels op voor chemisch geïnduceerde kernspin polarisatie bij afwezigheid van een magneetveld. Hoewel zij suggereren hetzelfde model te gebruiken als Closs, Trifunac en Kaptein, Oosterhoff is hun aanname van een tijdsafhankelijke hyperfijninteractie daarmee in strijd.

Charlton, J.L. en Bargon, J., 1971, Chem.Phys.Letters, 8, 442.

Kaptein, R. en Oosterhoff, L.J., 1969, Chem.Phys. Letters, 4, 195 en 214.

Closs, G.L. en Trifunac, A.D., 1970, J.Am.Chem.Soc., 92, 2138.

5. El-Sayed en medewerkers menen uit hun waarnemingen te kunnen concluderen dat de fosforescentie van chinoxaline en chinoline in een éénkristal van dureen, gepolariseerd is langs de lange as van het molekuul, maar in biphenyl loodrecht op het vlak. Uit hun experimentele gegevens is echter niet op te maken of hun conclusie in het geval van dureen gerechtvaardigd is.

Chaudhuri, N.K. en El-Sayed, M.A., 1966, J.Chem.Phys., 44, 3728.

Ziegler, S.M. en El-Sayed, M.A., 1970, J.Chem.Phys., 52, 3257.

6. Henry en Siebrand verklaren de waargenomen relatieve bevolkingssnelheden van de spincomponenten van de laagste fosforescerende triplettoestand T_o van naftaleen, bij intersystem crossing van $S_1 \rightarrow T_o$, door de aanwezigheid van een hoger gelegen triplet B_{2u}. Tegen deze argumentatie zijn twee bezwaren in te brengen.

Henry, B.R. en Siebrand, W., 1970, Chem.Phys.Letters, 7, 533.

7. De analyse van de microgolf faseverschuiver gegeven door Button en Lax is onjuist.

Lax, B. en Button, K.J., 1962, Microwave ferrites and ferrimagnetics, McGraw-Hill, p. 348 en 603.

8. Het is interessant op te merken dat Abragam voor de beschrijving van pure kern-quadrupool-echo experimenten een precessievergelijking gebruikt die identiek is aan de vergelijking van Feynman, Vernon en Hellwarth voor de beschrijving van maser-problemen.

Abragam, A., The principles of nuclear magnetism, 1961, Oxford Clarendon Press, p. 257 en p. 36.

Feynman, R.P., Vernon, F.L. en Hellwarth, R.W., 1957, J.Appl.Phys., 28, 49.

9. Ziekenhuizen en verpleeginrichtingen lenen geld tegen zeer hoge rente. Een financieringsbank voor de Nederlandse zieken- en verpleeghuizen zou hierin op goedkopere wijze kunnen voorzien.

J. Schmidt

2 juni 1971

Aan de nagedachtenis van mijn ouders

Aan Mieke, aan Wouter

C O N T E N T S

CHAPTER I

INTRODUCTION

The use of optical methods for the detection of radio frequency transitions between magnetic sublevels of excited states was first suggested by Brossel and Kastler in 1949. The technique is widely used in gases since Brossel and Bitter (1952) observed the transitions between sublevels of the $^3P_1$ excited state of mercury. The same method was applied to solids by Geschwind, Collins and Schawlow (1959) who found ESR transitions in the $\bar{E}(^2E)$ excited state of Cr^{3+} ions in Al_2O_3.

It has long been known that many organic molecules diluted in a solid matrix exhibit phosphorescence when irradiated with ultra violet light. On irradiation the molecule is brought from the singlet ground state to an excited singlet state and subsequently it relaxes via non-radiative processes into the lowest metastable triplet state T_o (fig. 1.1). The phosphorescence is emitted when the molecule decays in a radiative way from T_o, back to the ground state.

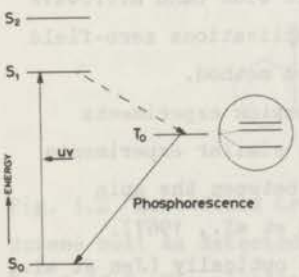

Fig. 1.1 The lower electronic states characteristic for a phosphorescent organic molecule. The components of the lowest triplet are shown in the circle.

This three level scheme was already proposed in 1933 by Jablonski as a phenomenological model and Lewis and Kasha (1944, 1945) identified the metastable state T_o with a triplet state. Contrary to singlet states, which are diamagnetic, the triplet state is characterized by two parallel spins and is paramagnetic. The value of the total spin angular momentum S = 1 and hence this state has three spin levels which in a molecular system are split in zero-magnetic field.

In 1958 Hutchison and Mangum succeeded in showing microwave ESR absorption in the phosphorescent triplet state of naphthalene diluted in a single crystal of durene. This successful experiment confirmed the triplet character of the phosphorescent state. From the anisotropy of the spectra in the applied magnetic field the magnetic axes and the zero-field splitting could be determined. Soon afterwards in 1959 van der Waals and de Groot observed the "$\Delta m = 2$" transitions of phosphorescent naphthalene diluted in a glass. From that time ESR experiments have become a standard technique for the study of phosphorescent triplet states.

In order to observe the transitions between the spin components of the triplet state in the absence of an external magnetic field a microwave spectrometer was constructed by Hutchison and his school (Erickson 1966, Hutchison 1967). The advantage of such a zero-field experiment would be that one is free of the anisotropy introduced by the magnetic field. Thus in principle it must be possible to work with randomly oriented molecules. This is important because often one has difficulties in preparing a suitable single crystal containing the phosphorescent substance. However the observation of the transitions via microwave detection presents serious technical problems. For instance it is very difficult to make a sensitive wide band microwave detection system. Apparently, owing to these complications zero-field spectroscopy has never become a generally applied method.

Of course one was aware of the optical detection experiments of Brossel and Kastler and it was suggested that similar experiments might be feasible for observing the transitions between the spin components of the lowest triplet state (de Groot et al., 1967). Attempts were made to detect the ESR transitions optically (Jen et al., 1967) with negative results until in 1967 Sharnoff observed the

"Δm = 2" transitions in naphthalene as a change in the intensity of its phosphorescence. Soon the "Δm = 1" transitions were also found in phosphorescent phenanthrene by Kwiram (1967) and by Schmidt, Hesselmann, de Groot and van der Waals (1967) in phosphorescent quinoxaline. In these experiments the measurement of phosphorescence is introduced to replace microwave detection in an ESR experiment that is conventional otherwise: a strong external field is applied to "tune" a transition between the spin levels to the frequency of the spectrometer.

The apparent advantages of optical methods over wide band microwave detection systems made us believe that the technique would be particularly suited for the observation of transitions between the spin levels in zero-magnetic field. Inspired by this idea we constructed a zero-field spectrometer employing a photomultiplier as the detection system. The first attempt was made on quinoxaline as a guest in a single crystal of durene. The experiment was successful: on the 24th of September 1968 we observed the 1187 MHz and 3641 MHz transitions through changes in the phosphorescence intensity. These recordings, displayed in fig. 1.2 were obtained at 1.52 K with the photomultiplier directly coupled to a recorder. Soon others took up the same technique and reported results on related systems (Tinti et al. 1969).

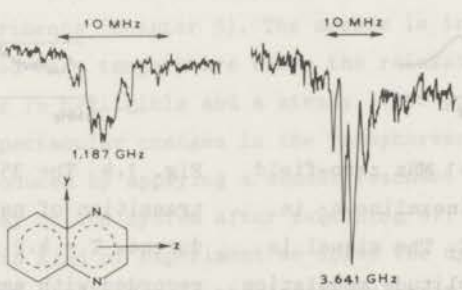

Fig. 1.2 Zero-field transitions of phosphorescent quinoxaline-h_6 in a durene host as detected in the output of the photomultiplier. T = 1.52 K. The signals correspond with a decrease in light intensity.

In the past two years we improved the sensitivity of the set-up and were able to observe zero-field transitions in many organic molecules. To illustrate the improvements made we again present in fig. 1.3 the 3641 MHz transition in quinoxaline. This time the line was recorded at 4.2 K with amplitude modulation of the microwave power together with phase-sensitive detection. Further a more efficient light gathering system was used. In fig. 1.4 we show the analogous transition in the related molecule naphthalene-d_8 , also as a guest in durene.

Although naphthalene and quinoxaline are very similar we see that the line shape in the latter molecule is much more complicated. We were able to explain this difference in structure by an analysis of the coupling of the electron spin to the nitrogen atoms in the aromatic ring (Schmidt and van der Waals 1969). This explanation will be one of our subjects of interest.

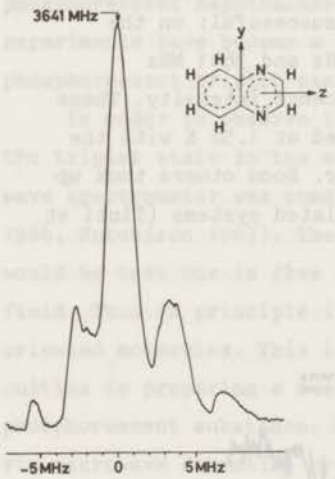

Fig. 1.3 The 3641 MHz zero-field transition of quinoxaline-h_6 in durene, T = 4.2 K. The signal is recorded with amplitude modulation of the microwave power at 160 Hz together with phase sensitive detection; RC time 1 s, sweep rate 0.1 MHz/s.

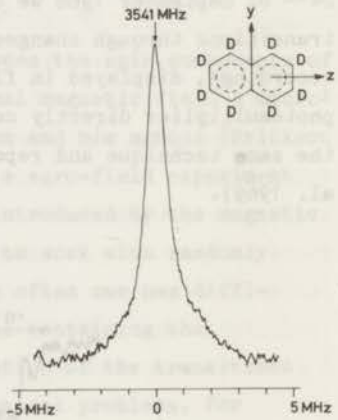

Fig. 1.4 The 3541 MHz zero-field transition of naphthalene-d_8 in durene, T = 4.2 K. The signal is recorded with amplitude modulation at 40 Hz together with phase sensitive detection; RC time 1 s, sweep rate 0.05 MHz/s.

The main purpose of the present thesis is to show the possibilities of zero-field spectroscopy with optical detection for the study of phosphorescent triplet states of organic molecules. This we shall do by presenting results of experiments on naphthalene, quinoline (1-azanaphthalene), quinoxaline (1,4-diazanaphthalene), each present as a guest in a single crystal of durene. We have chosen these three molecules because they are iso-electronic and have very similar phosphorescent triplet states. (In molecular orbital terminology the state arises by excitation of an electron from the highest bonding π m.o. to the lowest antibonding π^* m.o.) The differences in their properties due to the insertion of nitrogen atoms in the aromatic ring can be understood by simple theoretical models. Further they proved attractive for illustrating several aspects of zero-field spectroscopy.

Three different kinds of experiments will be discussed:

(1) Steady state experiments (Chapter 4). The system is irradiated continuously with u.v. light in the presence of a microwave field that is swept slowly through one of the resonant transitions. The conditions are so chosen that the response time of the triplet system is fast relative to a variation in microwave power produced by amplitude modulation of the oscillator. The concurrent variation in phosphorescence intensity is registered by a photomultiplier and one records the line shape of the zero-field transition by passing the signal from the photomultiplier through a phase sensitive detector.

(2) Transient experiments (Chapter 5). The system is irradiated during a limited period at a temperature where the relaxation between the spin components is negligible and a steady state population is established. Spectacular changes in the phosphorescence intensity may then be produced by applying a sudden resonant microwave field during the decay of the system after switching off the exciting light. From this kind of experiment we solve the dynamics of populating and depopulating of the individual spin levels.

(3) Coherence experiments (Chapter 6). The system is subjected to a strong resonant radio frequency field, with an amplitude exceeding the linewidth of the zero-field transition. In this situation the electron spins are coupled more strongly to the driving field than

with each other. One observes a modulation of the phosphorescence due to coherent coupling. From such experiments we hope to obtain detailed information about relaxation processes in phosphorescent triplet states.

CHAPTER 2

THE PHOSPHORESCENT TRIPLET STATE

2.1 MAGNETIC PROPERTIES

On the magnetic properties of the lowest phosphorescent triplet state of organic molecules some extensive review papers have been published (Hutchison 1967, van der Waals and de Groot 1967). Here we will only give a brief summary. One of the molecules of interest is quinoxaline and as an example we reproduce in fig. 2.1 its energy level scheme. On the left are the singlet ground state S_o and the lower excited singlet states. On the right the lowest (phosphorescent) triplet state T_o and the approximate position of a higher triplet. The labels at the left side of the levels give the orbital symmetries in C_{2v} (the symmetry group of quinoxaline).

When irradiated by ultra violet light at low temperature in a dilute crystalline matrix the molecule is excited from the ground state S_o into the singlet system. In general the molecule may return from the S_1 singlet state to the ground state by the emission of fluorescence or relax to the lowest triplet state T_o. From there it then decays to the ground state S_o either by emission of phosphorescence or via non-radiative processes. In the case of quinoxaline there is hardly any fluorescence and the relaxation into the triplet state must be relatively fast as compared with the radiative decay of S_1 which is of the order of 10^7 s^{-1}; the decay rate of T_o is about 3 s^{-1}.

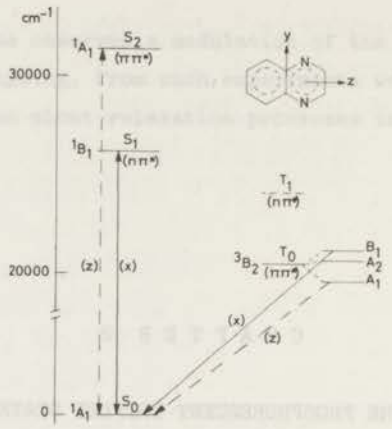

Fig. 2.1 The lower electronic states of quinoxaline. The labels at the left of the energy levels are orbital symmetries in C_{2v} , the other labels are total symmetries. The polarisation of the two symmetry allowed components of phosphorescence are indicated together with two singlet-singlet transitions from which they derive intensity.

Table 2.1

Character table of the group C_{2v}

C_{2v}		E	C_2	σ_y	σ_x
z	A_1	1	1	1	1
T_z	A_2	1	1	-1	-1
T_y x	B_1	1	-1	1	-1
T_x y	B_2	1	-1	-1	1

The splitting of the lowest triplet state in zero-magnetic field is mainly determined by the magnetic dipole-dipole interaction between the electron spins. The spin-orbit interaction contributes to a much

smaller extent although exceptions may occur, for instance in molecules with orbital degeneracy. The dipole-dipole interaction $\mathcal{H}_{ss}$ is given by

$$\mathcal{H}_{ss} = \gamma_e^2 \left(\frac{h}{2\pi}\right)^2 \sum_{i<j} \left\{ \frac{(\vec{s}_i . \vec{s}_j)}{r_{ij}^3} - \frac{3(\vec{s}_i . \vec{r}_{ij})(\vec{s}_j . \vec{r}_{ij})}{r_{ij}^5} \right\} \quad , \tag{2.1}$$

where $\vec{s}_i$ and $\vec{s}_j$ are the spin angular momentum operators of electrons i and j and $\vec{r}_{ij}$ gives the position of electron i with respect to electron j. To calculate this interaction energy one must integrate over the spatial distribution of the electrons in the phosphorescent state T_o. It has been shown by van Vleck (1951) that within the triplet multiplet the microscopic Hamiltonian (2.1) can be written as a phenomenological spin Hamiltonian in which only operators for the total spin angular momentum occur. By introducing $\vec{S} = \sum_i \vec{s}_i$ we obtain

$$\mathcal{H}_{ss} = \vec{S} \cdot \overline{\overline{T}} \cdot \vec{S} \quad , \tag{2.2}$$

where $\overline{\overline{T}}$ is the zero-field splitting tensor; its elements involve integrals of the operator (2.1) over the electron wave functions.

If an axis system x, y, z is chosen such that $\overline{\overline{T}}$ is diagonal and terms involving $S_x S_y$ etc. disappear, $\mathcal{H}_{ss}$ reduces to

$$\mathcal{H}_{ss} = - XS_x^2 - YS_y^2 - ZS_z^2 \quad . \tag{2.3}$$

The principal axes or spin axes of the tensor $\overline{\overline{T}}$ coincide with the molecular axes x, y, z if the molecule belongs to the symmetry group C_{2v} or to a symmetry group which contains C_{2v} as a subgroup. We assume in general that this occurs. If the symmetry of a molecule is lower and the spin axes do not coincide with the molecular axes we shall label the spin axes with primes.

The parameters X, Y and Z are the zero-field energies. Their magnitudes are determined by the energy of interaction of the magnetic moments of the electrons at distances comparable with the dimensions of the molecule. This gives rise to zero-field transitions of the order of 1000-10000 MHz. The triplet eigenfunctions T_x, T_y and T_z are linear combinations of the eigenfunctions of the S_z operator

$$T_x = \frac{1}{\sqrt{2}} \{ |-1\rangle - |+1\rangle \} \tag{2.4}$$

$$T_y = \frac{i}{\sqrt{2}} \{ |-1\rangle + |+1\rangle \} \qquad (2.5)$$

$$T_z = |0\rangle \quad . \qquad (2.6)$$

These functions have the property

$$S_x T_y = - S_y T_x = i T_z \quad , \text{ etc.} \quad ; \qquad (2.7)$$

$$S_u T_u = 0 \qquad u = x, y, z \quad . \qquad (2.8)$$

The spin function T_u is an eigenfunction of S_u with eigenvalue 0. In other words the triplet spin functions correspond to situations where the spin angular momentum vector lies in one of the three coordinate planes $x = 0$, $y = 0$ or $z = 0$. Moreover the triplet spin functions T_u transform as the u components of an axial vector (van der Waals and de Groot 1967). Hence in the symmetry group C_{2v} of quinoxaline T_x , T_y and T_z belong to the irreducible representations B_2 , B_1 and A_2 (see table 2.1). In this molecule where the spin axes coincide with the molecular axes the total symmetry of each of the triplet components is obtained as the direct product of orbital and spin symmetry. This is indicated in fig. 2.1 at the right of the triplet spin levels.

The magnetic properties of the phosphorescent triplet state have been studied very extensively with ESR spectroscopy. In such an experiment a static magnetic field H_o is applied and consequently a Zeeman term appears in the spin Hamiltonian

$$\mathcal{H} = \mathcal{H}_{ss} + \mathcal{H}_z = - XS_x^2 - YS_y^2 - ZS_z^2 - \gamma_e \frac{h}{2\pi} \vec{H}_o \cdot \vec{S} \quad , \qquad (2.9)$$

where γ_e is the magnetogyric ratio of the electron. The energies of the spin components depend on the direction and strength of $\vec{H}_o$ and are found from the secular equation;

$$\begin{vmatrix} X - \lambda & i\,\gamma_e \frac{h}{2\pi} H_o\, n & -i\,\gamma_e \frac{h}{2\pi} H_o\, m \\ -i\,\gamma_e \frac{h}{2\pi} H_o\, n & Y - \lambda & i\,\gamma_e \frac{h}{2\pi} H_o\, \ell \\ i\,\gamma_e \frac{h}{2\pi} H_o\, m & -i\,\gamma_e \frac{h}{2\pi} H_o\, \ell & Z - \lambda \end{vmatrix} = 0 \qquad (2.10)$$

where ℓ, m and n are the direction cosines of $\vec{H}_o$ with the spin axes x, y and z. The new eigenfunctions are linear combinations of T_x, T_y and T_z with coefficients depending on the value of $\vec{H}_o$ and on ℓ, m and n. If $\vec{H}_o$ is very large and along a direction $\vec{u}$ the Zeeman term dominates and the eigenfunctions approximate the eigenfunctions of S_u. The schematic diagram in fig. 2.2 shows the energy levels when $\vec{H}_o$ is parallel to x, y or z.

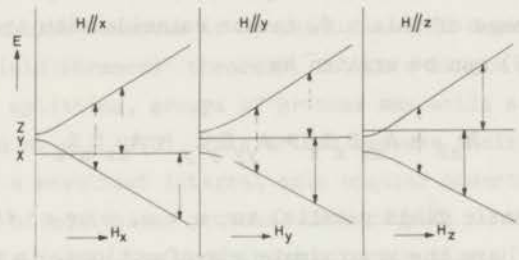

Fig. 2.2 The Zeeman splittings of a triplet state with a magnetic field along the principal axes x, y or z. The "$\Delta m = 1$" transitions are indicated by full lines and the "$\Delta m = 2$" transitions by broken lines.

ESR spectra are obtained by applying a microwave magnetic field. A time dependent term then appears in the spin Hamiltonian (2.9)

$$V(t) = - \gamma_e \frac{h}{2\pi} \vec{H}_1 \cdot \vec{S} \cos \omega t \quad . \qquad (2.11)$$

Transitions are induced between the spin states if the distance between two levels corresponds with the frequency of the microwave field. Three ESR transitions can be observed: one transition between the highest and lowest component similar to $\Delta m = 2$ in the atomic case and two transitions corresponding to $\Delta m = 1$ (fig. 2.2). The lines occur at different values of the magnetic field. Their positions depend on the orientation of $\vec{H}_o$ and the lines become stationary when $\vec{H}_o$ is parallel to one of the principal directions. From these stationary points the directions of the spin axes can be determined

and from the corresponding positions of the ESR lines one obtains the zero-field splitting parameters.

The ESR spectra are often split by the hyperfine interaction of the electron spin with nuclear spins. This interaction is described by a term in the spin Hamiltonian

$$\mathcal{H}_{HF} = \vec{S} \cdot \overline{\overline{A}} \cdot \vec{I} \quad , \tag{2.12}$$

where $\overline{\overline{A}}$ is the hyperfine tensor and $\vec{I}$ the nuclear spin operator. If the principal axes of this h.f. tensor coincide with the spin axes x, y and z , (2.12) can be written as

$$\mathcal{H}_{HF} = A_{xx} S_x I_x + A_{yy} S_y I_y + A_{zz} S_z I_z \quad . \tag{2.13}$$

In a large magnetic field parallel to $u = x, y$ or z the eigenfunctions of S_u are the approximate eigenfunctions. In this representation one of the h.f. terms of (2.13) is diagonal and gives a first order splitting of the electron spin levels. From the resulting splitting of the ESR lines in the three principal directions one then finds A_{xx} , A_{yy} and A_{zz} .

Let us now consider the situation in zero field. Transitions then may be induced between the spin states T_x , T_y and T_z by the same time-dependent term (2.11) as in normal ESR experiments. The transitions are linearly polarized in the x, y or z direction as can be seen from the properties of the spin functions T_x , T_y and T_z (2.7).

An important advantage of zero-field spectroscopy is that the anisotropy introduced by the static magnetic field and the corresponding scrambling of the zero-field functions is absent. The splitting of the electron spin states is independent of the orientation of the molecule in space. Hence in principle it is not necessary to work with oriented molecules in a single crystal. In order to induce the transitions one merely needs a component of the magnetic microwave field along the corresponding direction of polarisation. The directions of the spin axes however, can only be obtained from the polarisation of the resonant microwave transition. One would expect this to be less accurate than via an ESR experiment

in which the directions of the spin axes are determined with the help of a static magnetic field.

The problem of the line shapes will be discussed in chapter 4. Here we merely note that the zero-field lines cannot show the familiar hyperfine structure of ordinary ESR spectra: because of the relations (2.7 and 2.8) the h.f. term (2.12) can only give matrix elements between different zero-field states and no first order splittings will occur in the electron spin levels. If a single nuclear spin $I = \frac{1}{2}$ is present one even expects no splitting at all because a state having half integral angular momentum is at least two-fold degenerate in zero-magnetic field (Kramers' theorem). Though a single proton does not lead to any splitting, groups of protons may still affect the line shape (Hutchison et al. 1970). This arises because their combined states may have a resultant integral spin angular momentum (e.g. $I = 0$ or 1 for a pair of equivalent protons) that couples to the electron spin. In order to reduce the contribution to the line width due to the protons, we have also studied a number of deuterated molecules including quinoxaline-d_6.

2.2 RADIATIVE PROPERTIES

The radiative properties of the spin components of the phosphorescent triplet state are determined by the spin-orbit coupling in the molecule. This interaction mixes singlets with triplets and allows electric dipole transitions to occur between the lowest triplet state and the singlet ground state. Hence the phosphorescence appears to be stolen from allowed singlet-singlet and triplet-triplet transitions. The mixing is very selective because spin-orbit interaction only gives matrix elements between singlet and triplet states of the same total symmetry. As a result, the radiative transition probabilities k_u^r ($u = x, y, z$) of the three spin components of a phosphorescent triplet state in general are different. For instance in quinoxaline (fig. 2.1) one might expect the top level B_1 and the lowest level A_1 to decay via x and z polarized phosphorescence,

respectively[†]. Our previous experiments (de Groot et al. 1968) as well as the results of chapter 5 show that the phosphorescence originates predominantly from the top level.

In the optical detection technique one makes use of these differing radiative decay rates. When magnetic dipole transitions are induced between two components of the triplet state the equilibrium populations of the levels are affected and a change in the phosphorescence intensity occurs. This effect will be more pronounced the larger the differences in radiative decay rates of the individual levels. Further, one expects that it is advantageous to work at low temperature (liquid helium) in order to obtain large differences in the populations of the spin levels.

The importance of this new approach is that the detection of the zero-field transitions is removed from the microwave region to detecting optical photons. From an experimental point of view this offers a considerable advantage because it circumvents the complications inherent in microwave detection techniques. It is well known that in normal ESR spectrometers where microwave cavities and bridges are used the detection sensitivity is strongly frequency dependent. Consequently one is forced to work at fixed frequency and in order to observe the ESR lines one varies the magnetic field. In zero-field spectrometers one must vary the frequency. Hence in the instrument constructed by Erickson (1966) a tunable cavity and microwave bridge is employed. The optical detection technique is free from these difficulties and hence attractive to apply, not only in cases where a magnetic field is present but particularly for the detection of zero-field transitions. Indeed such a zero-field spectrometer with optical detection is relatively simple as we shall see in the next chapter where experimental details are given.

[†] In order to keep the discussion simple we neglect the breaking of electronic selection rules due to vibronic coupling. Although non-totally symmetric vibrations are important in the structure of the $T_o \longrightarrow S_o$ optical spectrum (El-Sayed et al. 1970), they contribute only a small fraction to the total intensity of the phosphorescence.

CHAPTER 3

EXPERIMENTAL

3.1 THE SPECTROMETER

The schematic diagram of the experimental arrangement used for the study of the zero-field transitions is shown in fig. 3.1. The microwave source consists of a Hewlett Packard HP 8690 B sweep oscillator which can receive each of the HP 8690 series Backward Wave Oscillators (BWO's) as a plug-in. With this combination we cover the frequency range of 100 to 12400 MHz, where the BWO's provide about 100 mW of microwave power with a residual frequency modulation of about 30 kHz. The microwave power is fed through coaxial lines via an adjustable attenuator and a circulator to a helix acting as our resonator. The power reflected from the open ended helix is directed through the circulator to a termination. A small fraction is going via a directional coupler to a frequency meter.

The sample is mounted against the end of a quartz light pipe in a small teflon container with a quartz window. The light pipe projects into the helix and can if necessary be moved up and down to bring the sample to a position of maximum r.f. field. The whole assembly is placed in an optical liquid helium dewar with quartz windows in the bottom through which the u.v. irradiation is applied. Small holes in the teflon container permit the liquid helium to pass freely around the crystal in order to provide the cooling necessary to prevent heating of the crystal by the exciting radiation.

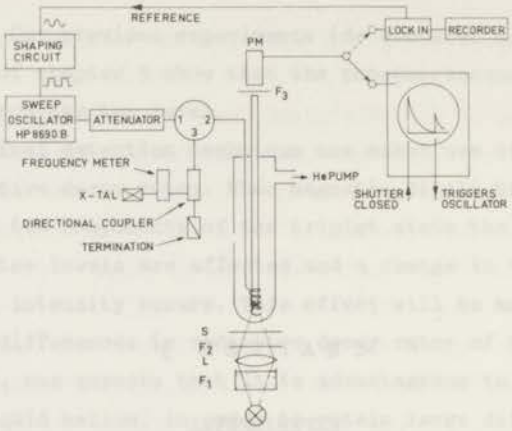

Fig. 3.1 Schematic diagram of the zero-field spectrometer with optical detection.

The light source is a Philips SP 1000 Watt watercooled super-high pressure mercury arc. The exciting light passes through a solution filter F_1 and a glass filter F_2. The phosphorescence of the sample is observed by a photomultiplier (EMI 9524 B) via the quartz light pipe and a filter F_3. The filter F_1 usually was a solution of 240 g/l $NiSO_4.6H_2O$ plus 45 g/l $CoSO_4.7H_2O$ and F_2 a Chance Pilkington OX-7 or Schott und Gen. UG-5 glass filter. F_3 consisted of a pair of Optics Technology Inc. variable bandpass interference filters, transmitting between 450 and 550 nm.

In the steady state experiments the sample is continuously irradiated. In the first successful experiment on quinoxaline displayed in fig. 1.2 the signals were obtained at 1.52 K with d.c. detection at the photomultiplier output. This detection method is not the most sensitive one, because the signal-to-noise ratio is severely deteriorated by low frequency instabilities of the light source. Instead one would prefer to detect the changes in phosphorescence intensity by a "lock-in" amplifier at a frequency where these instabilities are negligible. In order to obtain the response time in the triplet system necessary for the use of modulation techniques the temperature was increased to 4.2 K. At this temperature the relaxation is so fast that amplitude modulation of the microwave power results in changes in the

phosphorescence intensity at the same frequency. The output of the photomultiplier is then connected to a Princeton Applied Research (PAR) model 220 "lock-in" amplifier coupled to a recorder. The reference frequency of the "lock-in" is used to drive the amplitude modulation of the microwave source. The modulation frequency that can be used depends on the dynamics of the triplet system and usually is in the range of 20-400 Hz. The zero-field spectra are obtained by slowly sweeping the microwave frequency through resonance. The modulated part of the phosphorescence is phase-sensitive detected by the "lock-in" and its output displayed on the recorder. The 3641 MHz transition in quinoxaline shown in fig. 1.3 has been obtained in this way. The improvement in signal-to-noise ratio compared with the d.c. detection method (fig. 1.2) is mainly due to the "lock-in" detection and partly to a more efficient light gathering system.

The helix is described in several textbooks on microwave techniques (Watkins, Pierce) and also for application to magnetic resonance by Webb (1962). Expressions are given for the electric and magnetic field configuration in the physical abstraction known as the "sheath" helix. We will not give them here because our helix is far from ideal and a knowledge of the exact field configuration is not so important for our optical detection experiments. It is enough to know that a microwave magnetic field is present within the coil. Because the mode propagating along the wire is basically the same as in the coaxial line it is possible to match the helix over a wide frequency range. At the open end the wave is reflected and a standing wave exists. The dimensions of our helix are: thickness of the wire 0.5 mm, inner diameter 4.4 mm, distance between the wires 1 mm, number of turns 6.

The attractive feature of this resonator for optical experiments is its open structure and for zero-field work its wide band operation. We may expect however that the microwave magnetic field over a sample of 10-20 mm^3 will be rather inhomogeneous in amplitude and especially in direction.

In the transient experiments a change in phosphorescent light intensity is induced during the decay of the triplet state. In these experiments the output of the photomultiplier is connected directly to a Tektronix 549 storage oscilloscope. The exciting light is shut off

by a mechanical shutter (Synchro-Compur) with a closure time of 0.2 ms. The closing of the shutter triggers the base line of the oscilloscope while a delayed pulse subsequently triggers a sweep of the BWO through the resonance frequency of a zero-field transition. In this experiment no amplitude modulation of the microwave power is applied.

3.2 THE SYSTEMS STUDIED

We have studied quinoline-h_7 and -d_7, quinoxaline-h_6 and -d_6 and naphthalene-d_8 as dilute solutions in single crystals of durene. The "guests" replace durene molecules and can be considered as an "oriented gas". The durene crystal is monoclinic with $\beta = 113.3^\circ$ and there are two molecules per unit cell (Robertson 1933).

In the appendix details are given about the origin of the chemicals, preparation of the crystals and mass spectrometric analysis of the "perdeutero" compounds. As mentioned in section 2.1 the deuterated isomers have narrower zero-field transitions than the hydro-compounds. An additional advantage of the former is their greater phosphorescence intensity which arises because radiationless deactivation of the triplet state is reduced on D substitution (Hutchison and Mangum 1960, Robinson and Frosch 1963). The average degree of deuteration of the samples (d/h ratio) in all cases exceeded 96% but even then some 15-20% of the molecules contain one or more H atoms.

In naphthalene the spin levels T_x , T_y and T_z lie in order of increasing energy and in quinoline and quinoxaline the ordering is the same (Hornig and Hyde 1963, Schmidt et al. 1970) (fig. 3.2). The three molecules are approximately planar and hence one of the spin axes, in our convention the x-axis must be perpendicular to the molecular plane. In quinoxaline and naphthalene the in-plane axes are by symmetry constrained to lie along and perpendicular to the central bond, but for quinoline this is no longer true. Experimentally it is observed (Vincent and Maki 1965) that the spin axes x' and y' deviate by 13° from the directions x and y.

The phosphorescence spectra of the three molecules are very similar and cover a broad region, roughly between 450 and 550 nm. In

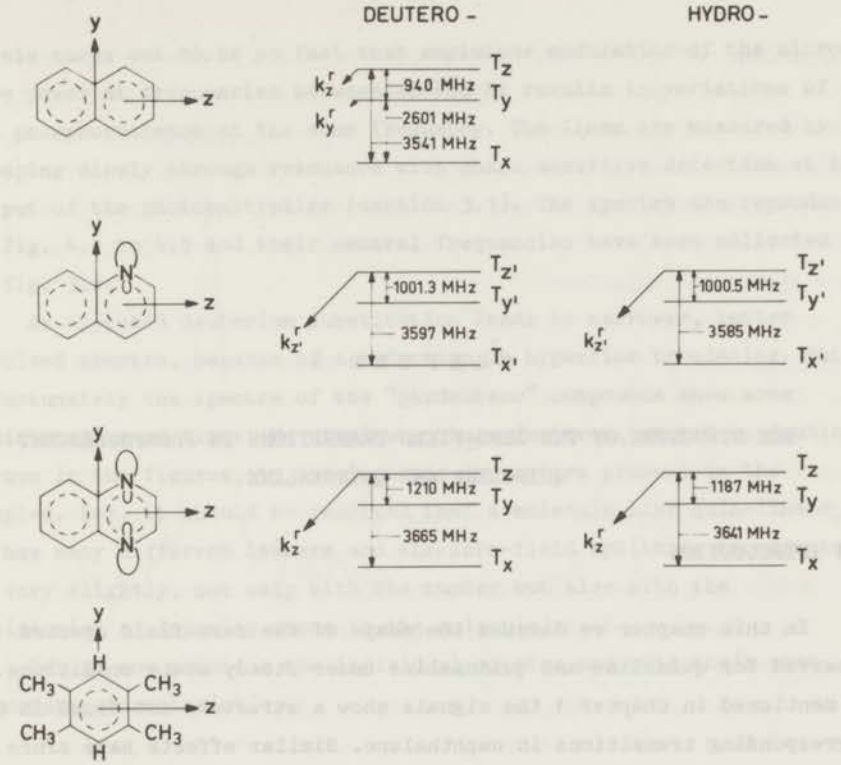

Fig. 3.2 The positions of the spin components of the lowest triplet states of naphthalene-d_8 , quinoline-d_7 and -h_7 , and quinoxaline-d_6 and -h_6. The symbols k_z^r and k_y^r stand for the radiative decay rates of T_z and T_y. The arrows indicate the dominant channels of radiative decay. The frequencies of the transitions observed at 4.2 K are given in MHz. The frequencies refer to the highest point of deflection of the recorded line.

durene the 0-0 band of quinoxaline is found at 464 nm, (Chaudhuri and El-Sayed 1966), of quinoline at 458 nm (Ziegler and El-Sayed 1970) and of naphthalene-d_8 at 467 nm. By filtering the phosphorescence is easily separated from the exciting light which is usually between 250-320 nm.

CHAPTER 4

THE STRUCTURE OF THE ZERO-FIELD TRANSITIONS IN PHOSPHORESCENT QUINOLINE AND QUINOXALINE

4.1 INTRODUCTION

In this chapter we discuss the shape of the zero-field spectra observed for quinoline and quinoxaline under steady state conditions. As mentioned in chapter 1 the signals show a structure not found in the corresponding transitions in naphthalene. Similar effects have since been found by other groups in related aza-aromatic molecules (Tinti et al. 1969).

In section 4.2 we first present experimental results of a systematic study of the spectra for quinoline and quinoxaline. Then in section 4.3 we turn to the theoretical interpretation of the line shapes based on the known hyperfine and quadrupole interaction with the N^{14} nuclei. In this model we neglect hyperfine interaction with the protons. In the conclusion we consider some general aspects of hyperfine interaction in zero-field. Particularly we shall indicate the effect of h.f. interaction with groups of protons, a subject treated extensively by Hutchison, Nicholas and Scott (1970).

4.2 RESULTS OF STEADY STATE EXPERIMENTS

The zero-field transitions of present interest have all been measured at 4.2 K. At this temperature relaxation between the spin

levels turns out to be so fast that amplutude modulation of the microwave power at frequencies between 20-400 Hz results in variations of the phosphorescence at the same frequency. The lines are measured by sweeping slowly through resonance with phase sensitive detection at the output of the photomultiplier (section 3.1). The spectra are reproduced in fig. 4.1 to 4.5 and their central frequencies have been collected in fig. 3.2.

As expected deuterium substitution leads to narrower, better resolved spectra, because of a reduction in hyperfine broadening. But unfortunately the spectra of the "perdeutero" compounds show some additional broad lines. We attribute these features, marked by double arrows in the figures, to the isotopic impurities present in the samples. For, it should be realized that a molecule like quinoline-d_6-h_1 has many different isomers and the zero-field splitting is expected to vary slightly, not only with the number but also with the position(s) of impurity atoms in the molecule.

Let us now consider the individual spectra and note their most important characteristics.

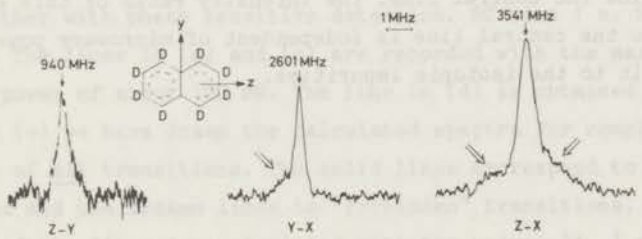

Fig. 4.1 The optically detected zero-field transitions of naphthalene-d_8 in durene. T = 4.2 K. The spectra are recorded with amplitude modulation at 40 Hz together with phase sensitive detection. RC time 1 s. Sweep rate 0.05 MHz/s. The double arrows indicate lines which we attribute to partly deuterated molecules.

Naphthalene Only the deuterated isomer has been studied. From experiments by Sixl and Schwoerer (1970) on naphthalene-h_8 it turns out that the top level T_z is the most radiative; $k_z^r > k_y^r > k_x^r$. At 4.2 K we observe all three transitions (fig. 4.1). The three lines show no structure and are considerably narrower than the corresponding transitions in naphthalene-h_8 found by Hutchison et al. (1970) in a microwave absorption experiment.

Quinoline In quinoline the top level is by far the most radiative and only two of the transitions are found: Z - Y and Z - X.

We discovered a remarkable variation of some of the transitions with microwave power. This is shown in fig. 4.2 for the Z - X transition of quinoline-h_7, where at high power two satellites appear around the central line at a distance of about 3 MHz. The Z - Y transition consists of one line and no satellites were observed.

Secondly, when working at low power level the central lines in quinoline-d_7 show structure; the Z - Y line at the left in fig. 4.3 is split into two components separated by 0.75 MHz and with an intensity ratio of 1:2, while the central Z - X line at the right shows a shoulder at the low frequency side. In the perdeutero compound the satellites in the Z - X transition are more difficult to see but instead a strong broad signal indicated by a double arrow is present 2.4 MHz below the central line. The intensity ratio of this signal relative to the central line is independent of microwave power and we attribute it to the isotopic impurities.

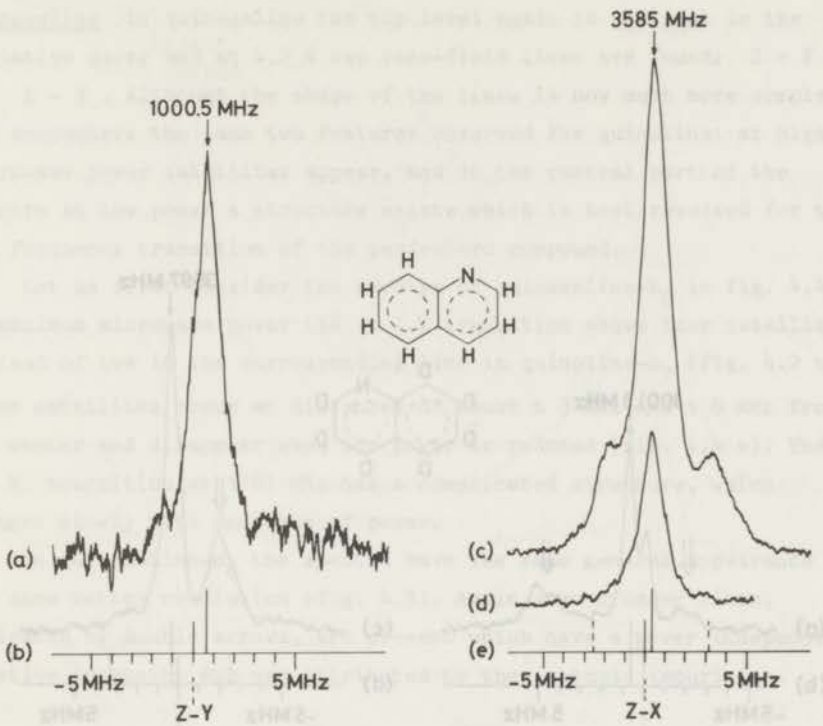

Fig. 4.2 The optically detected zero-field transitions Z - Y and Z - X of quinoline-h_7 in durene. T = 4.2 K. Amplitude modulation at 80 Hz together with phase sensitive detection. RC time 1 s. Sweep rate 0.1 MHz/s. The lines in (a) and (c) are recorded with the maximum microwave power of about 100 mW. The line in (d) is obtained with 1 mW. In (b) and (e) we have drawn the calculated spectra for complete saturation of all transitions. The solid lines correspond to "allowed" transitions and the broken lines to "forbidden" transitions. The positions of the lines are calculated with the values $|A_{xx}|$ = 22 MHz, Z - Y = 1000.5 MHz, $\varepsilon_z - \varepsilon_y$ = 3.0 MHz.

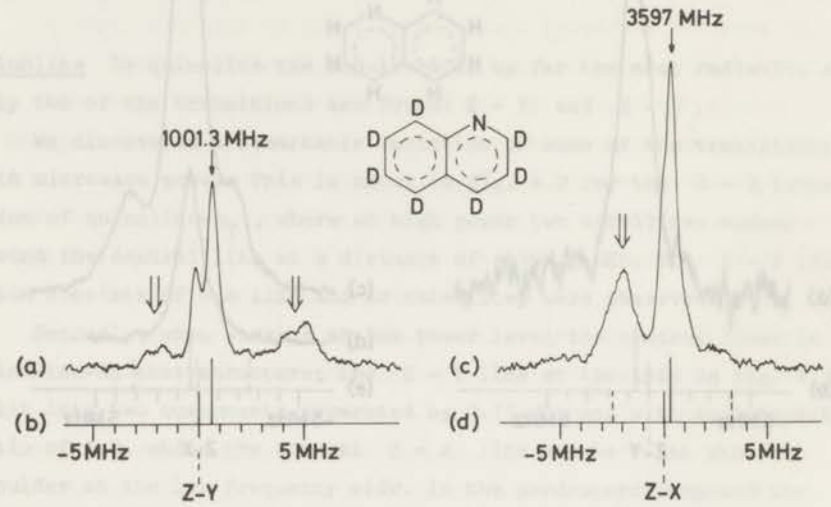

Fig. 4.3 The optically detected zero-field transitions Z - Y and Z - X of quinoline-d_7 in durene. T = 4.2 K. Amplitude modulation at 80 Hz together with phase sensitive detection. RC time 1 s. Sweep rate 0.05 MHz/s. The spectra (a) and (c) have been recorded with a microwave power of about 1 mW (20 db below maximum power). In (b) and (d) we have redrawn the calculated spectrum of fig. 4.2. The double arrows indicate lines which we attribute to partly deuterated molecules.

Quinoxaline In quinoxaline the top level again is dominant in the radiative decay and at 4.2 K two zero-field lines are found: Z - Y and Z - X . Although the shape of the lines is now much more complex, one encounters the same two features observed for quinoline: at high microwave power satellites appear, and in the central part of the spectra at low power a structure exists which is best resolved for the low frequency transition of the perdeutero compound.

Let us first consider the spectra of quinoxaline-h_8 in fig. 4.4. At maximum microwave power the Z - X transition shows four satellites instead of two in the corresponding line in quinoline-h_7 (fig. 4.2 c). These satellites occur at distances of about ± 3 MHz and ± 6 MHz from the center and disappear when the power is reduced (fig. 4.4 e). The Z - Y transition at 1187 MHz has a complicated structure, which changes slowly with decrease of power.

In quinoxaline-d_6 the spectra have the same general appearance but show better resolution (fig. 4.5). Again some broader lines, indicated by double arrows, are present which have a power independent relative intensity and are attributed to the isotopic impurities.

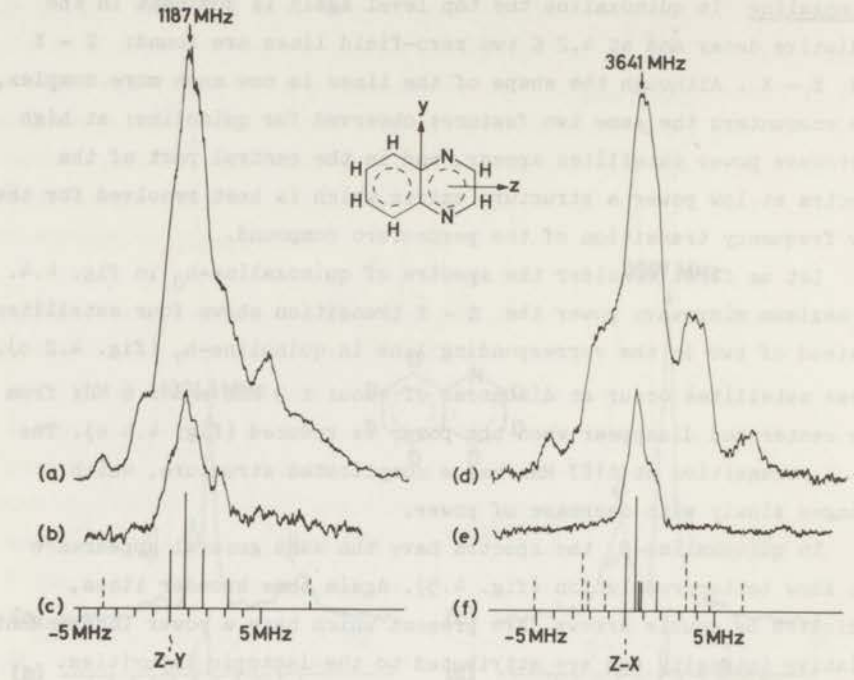

Fig. 4.4 The optically detected zero-field transitions Z - Y and Z - X of quinoxaline-h_6 in durene. T = 4.2 K. Amplitude modulation at 160 Hz together with phase sensitive detection. RC time 1 s. Sweep rate 0.1 MHz/s. The spectra (a) and (d) have been recorded with the maximum microwave power of 100 mW; the lines in (b) and (e) with 0.5 mW and 10 μW respectively. In (c) and (f) we have drawn the calculated spectrum for complete saturation of all transitions. The solid lines correspond to "allowed" transitions and the broken lines to "forbidden" transitions. The positions of the lines have been calculated with $|A_{xx}|$ = 21.88 MHz, Z - Y = 1187 MHz, $\varepsilon_z - \varepsilon_y$ = 3.0 MHz.

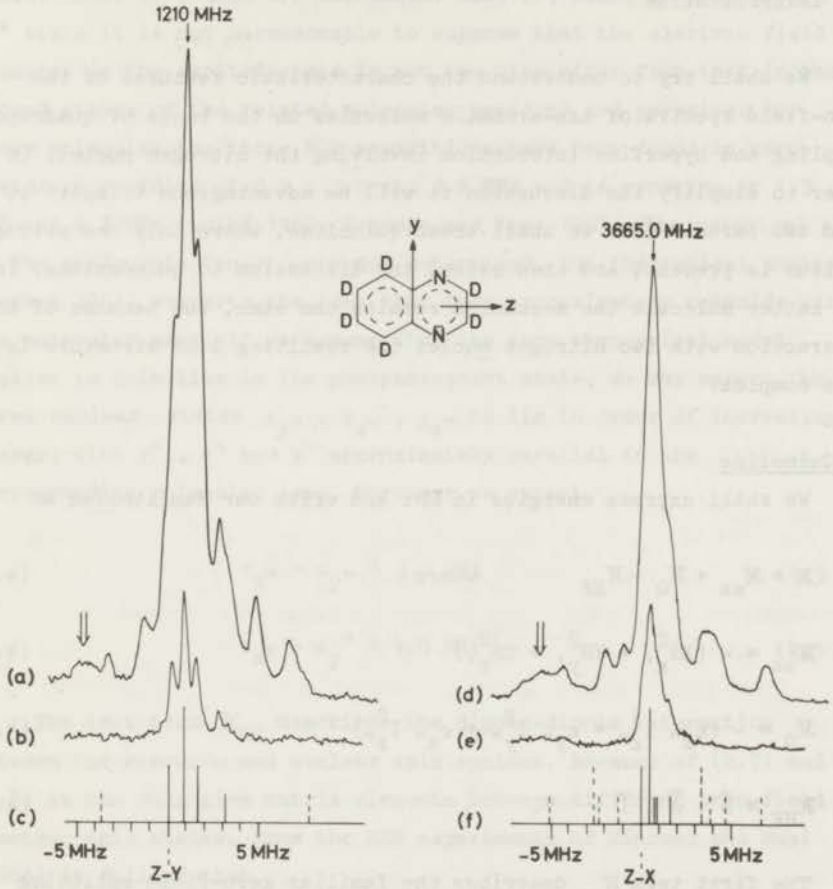

Fig. 4.5 The optically detected zero-field transitions Z - Y and Z - X of quinoxaline-d_6 in durene. T = 4.2 K. Amplitude modulation at 160 Hz together with phase sensitive detection. RC time 1 s. Sweep rate 0.1 MHz/s. The spectra (a) and (d) have been recorded with maximum microwave power at 100 mW; the spectra (b) and (e) with 0.5 mW and 100 μW, respectively. In (c) and (f) we have reproduced the calculated spectrum of fig. 4.4. The double arrows indicate lines which we attribute to partly deuterated molecules.

4.3 INTERPRETATION

We shall try to understand the characteristic features of the zero-field spectra of aza-aromatic molecules on the basis of quadrupole coupling and hyperfine interaction involving the nitrogen nuclei. In order to simplify the discussion it will be advantageous to split it into two parts. First we shall treat quinoline, where only one nitrogen nucleus is present, and then extend the discussion to quinoxaline. In the latter molecule the mechanism remains the same, but because of the interaction with two nitrogen nuclei the resulting line structure is more complex.

A. Quinoline

We shall express energies in MHz and write our Hamiltonian as

$$\mathcal{H} = \mathcal{H}_{ss} + \mathcal{H}_{Q} + \mathcal{H}_{HF} \qquad \text{where} \tag{4.1}$$

$$\mathcal{H}_{ss} = -\left(XS_{x'}^2 + YS_{y'}^2 + ZS_{z'}^2\right) \tag{4.2}$$

$$\mathcal{H}_{Q} = -\left(\varepsilon_{x''} I_{x''}^2 + \varepsilon_{y''} I_{y''}^2 + \varepsilon_{z''} I_{z''}^2\right) \tag{4.3}$$

$$\mathcal{H}_{HF} = \vec{S} \cdot \overline{\overline{A}} \cdot \vec{I} \quad . \tag{4.4}$$

The first term $\mathcal{H}_{ss}$ describes the familiar zero-field splitting of the electron spin system. We know from the ESR experiments of Vincent and Maki (1965) that the in-plane spin axes deviate by $+13^{\circ}$ or -13° from the molecular axes. In order to distinguish the spin axes we designate them by primes.

The second term $\mathcal{H}_{Q}$ describes the quadrupole splitting of the spin states of the nitrogen nuclei in the principal axes system x" , y" , z" determined by the electric field gradient at the nitrogen nucleus. $\mathcal{H}_{Q}$ is diagonalized by nuclear spin functions χ_k (k = x" , y" , z"). These nuclear spin functions for $I = 1$ obey the same relations as the $S = 1$ electron spin functions T_u (u = x' , y' , z') (2.7 and 2.8).

For the present purpose one would need the eigenenergies and principal axes directions of $\mathcal{H}_{Q}$ for quinoline in its phosphorescent

state. These of course are not known. However, since we deal with a $\pi\pi^*$ state it is not unreasonable to suppose that the electric field gradient in the excited state is not too dissimilar from that in the ground states of the related molecules pyridine and pyrazine. For these molecules the three NQR transitions have been found in zero-field: in pyridine at 0.9 , 3.0 and 3.9 MHz and in pyrazine at 1.3 , 3.0 and 4.3 MHz (Guibé 1962, Schempp and Bray 1967). The principal axes of the quadrupole tensor were not determined, but theoretical analysis (Lucken 1961) supports the idea that they approximately coincide with the molecular axes. If we assume that the same theoretical model applies to quinoline in its phosphorescent state, we may expect the three nuclear states $\chi_{y''}$, $\chi_{z''}$, $\chi_{x''}$ to lie in order of increasing energy, with y" , z" and x" approximately parallel to the corresponding molecular axes. Moreover we expect

$$\varepsilon_{z''} - \varepsilon_{y''} \approx 3.0 \text{ MHz} \qquad (4.5\text{ a})$$

$$\varepsilon_{x''} - \varepsilon_{y''} \approx 4.0 \text{ MHz} \qquad (4.5\text{ b})$$

The last term $\mathcal{H}_{HF}$ describes the dipole-dipole interaction between the electron and nuclear spin systems. Because of (2.7) and (2.8) it can only give matrix elements between different zero-field electron spin states. From the ESR experiments of Vincent and Maki (1965) it follows that

$$|A_{xx}| \approx 22 \text{ MHz} \quad , \quad |A_{yy}| \leq 4 \text{ MHz} \quad , \quad |A_{zz}| \approx 4.4 \text{ MHz} \; . \qquad (4.6)$$

The main features of the zero-field spectra of quinoline and later of quinoxaline can be understood by making two simplifying assumptions suggested by the above information about $\mathcal{H}_{ss}$, $\mathcal{H}_{Q}$ and $\mathcal{H}_{HF}$.

(a) The principal axes of $\mathcal{H}_{ss}$, $\mathcal{H}_{Q}$ and $\mathcal{H}_{HF}$ all are assumed parallel to the molecular axes x, y and z.

(b) Because of the great disparity between the elements (4.6) the hyperfine interaction further may be approximated by its leading term

$$\mathcal{H}_{HF} = A_{xx} S_x I_x \quad . \tag{4.7}$$

We shall show later that these approximations are less restrictive than they may seem at first sight.

The spin functions which diagonalize $\mathcal{H}_{ss} + \mathcal{H}_Q$ are $T_u X_k$ (where now u and $k = x, y, z$). Hence if magnetic hyperfine interaction were absent, each of the three electron spin levels would consist of three components with energies $U + \varepsilon_k$ (where $U = X, Y, Z$ and $k = x, y, z$) as indicated in fig. 4.6.

The zero-field transitions are induced by a time dependent Hamiltonian of the following form

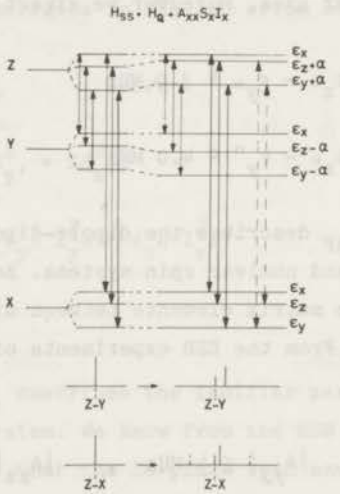

Fig. 4.6 Energy level scheme of the lowest triplet state of quinoline. Each of the three zero-field electron spin states is split into three levels by the quadrupole splitting of the N^{14} nucleus. At the right some of the levels are shifted further by second order hyperfine interaction, $\alpha = A_{xx}^2 / (Z-Y)$. At the bottom the spectrum that results has been indicated. The "allowed" transitions are indicated by full lines and the "forbidden" ones by broken lines.

$$V(t) = \frac{1}{2\pi} (-\gamma_e \vec{S} - \gamma_n \vec{I}) \cdot \vec{H}_1 \cos \omega t \quad , \qquad (4.8)$$

where we have added a term for the interaction of the microwave magnetic field with the magnetic moment of the nucleus (the factor 2π arises because the magnetogyric ratios are in radians.sec^{-1}.gauss^{-1}). For frequencies in the neighbourhood of one of the zero-field splittings only the electron spin part will contribute significantly to the transition probability. Without the hyperfine term $\mathcal{H}_{HF}$ the observed signal would correspond to transitions of the type $T_z X_k \leftarrow T_y X_k$ and $T_z X_k \leftarrow T_x X_k$, where the electron spin state is changed and the nuclear state conserved. In this situation the three nuclear components of each electron transition would coalesce at the single frequencies $Z - Y$ and $Z - X$, because the nuclear quadrupoles do not "feel" the electron spins.

When next considering the hyperfine term $A_{xx} S_x I_x$ we see that because of (2.7) and (2.8) it cannot affect the T_x manifold but it will give matrix elements between the states $T_z X_z$ and $T_y X_y$, and between $T_z X_y$ and $T_y X_z$. In table 4.1 we give the resulting spin functions to first order in $|A_{xx}|$ and the eigenenergies to second order. The influence on the shape of the $Z - X$ and $Z - Y$ transition is twofold (see fig. 4.6).

(a) The three "allowed" transitions in each zero-field line, in which the nuclear spin state is conserved and which coincide if $\mathcal{H}_{HF}$ is neglected, will be split by the second order energy shift $\alpha = A_{xx}^2 / (Z-Y) \approx 0.4$ MHz. As a result in the $Z - X$ transition one line will occur at $(Z - X)$ and the other two at $(Z - X) + \alpha$. In the $Z - Y$ transition one at $(Z - Y)$ and two at $(Z - Y) + 2\alpha$.

These splittings are indeed observed in the spectra of quinoline-d_7 (fig. 4.3). The "allowed" $Z - Y$ line is split into two components with an intensity ratio 1:2. In the "allowed" $Z - X$ line the second order energy splitting is halved and the transition only has a shoulder at the low frequency side. From the separation of 0.75 MHz observed for the two components of the "allowed" $Z - Y$ line we calculate $|A_{xx}| = 19.4$ MHz instead of the value $|A_{xx}| = 22$ MHz derived from a high-field ESR spectrum by Vincent and Maki (1965).

Table 4.1

The spin functions of quinoline to first order and the eigenenergies to second order. $\alpha = A_{xx}^2/(Z-Y)$, $\beta = A_{xx}/(Z-Y)$.

First order eigen functions	Second order energies
$T_z\chi_x$	$Z + \varepsilon_x$
$T_z\chi_z - \beta\, T_y\chi_y$	$Z + \varepsilon_z + \alpha$
$T_z\chi_y + \beta\, T_y\chi_z$	$Z + \varepsilon_y + \alpha$
$T_y\chi_x$	$Y + \varepsilon_x$
$T_y\chi_z - \beta\, T_z\chi_y$	$Y + \varepsilon_z - \alpha$
$T_y\chi_y + \beta\, T_z\chi_z$	$Y + \varepsilon_y - \alpha$
$T_x\chi_x$	$X + \varepsilon_x$
$T_x\chi_z$	$X + \varepsilon_z$
$T_x\chi_y$	$X + \varepsilon_y$

(b) "Forbidden" lines will occur in the Z - X transition, which are displaced by $\pm(\varepsilon_z - \varepsilon_y) \simeq 3$ MHz with respect to the allowed line at $(Z-Y) + \alpha$ and which have relative transition probabilities of $\beta^2 = A_{xx}^2/(Z-Y)^2 \simeq 4 \times 10^{-4}$. These satellites correspond with a nuclear flip in addition to an electronic transition (fig. 4.6 and table 4.1).

In the spectrum of quinoline-h_7 shown in fig. 4.2 we observe that for maximum microwave power two satellites indeed occur in the high frequency transition. These satellites are displaced by about ± 3 MHz and disappear upon reduction of microwave power.

The low frequency Z - Y transition at 1000.5 MHz does not show satellites even at maximum power, just as expected from our model.

In the spectrum of quinoline-d_7 the satellites around the Z - X line unfortunately are obscured by the lines due to isotopic impurities like quinoline-d_6-h_1. Hence for the study of the satellites they are less suited then the hydro compound and in fig. 4.3 we have presented only low power recordings of quinoline-d_7 in order to show the splitting of the "allowed" line.

Before turning to the discussion of quinoxaline we shall make two remarks about the validity of the approximations (a) and (b). First, the approximation (b) is better than one would expect from the inequality of the tensor elements (4.6) alone, because $|A_{yy}|$ and $|A_{zz}|$ give matrix elements between spin states that have energy differences two and three times larger than Z - Y. For instance, the two corresponding terms that have been neglected in the energy expression, $|A_{yy}|^2/(Z-X)$ and $|A_{zz}|^2/(Y-X)$ are less than 0.01 MHz. Second, if only $|A_{xx}|$ is considered with x perpendicular to the molecular plane, then the direction of the in-plane principal axes does not affect the line shapes: the term $A_{xx}S_xI_x$ only gives matrix elements between T_zX_u and T_yX_v and this interaction does not depend on the orientation of the in-plane principal axes which need not to be coincident for the different tensors.

B. Quinoxaline

In this molecule two equivalent nitrogen atoms are present and hence we have to extend the last two terms in our Hamiltonian (4.1)

$$\mathcal{H}_Q = -(\varepsilon_x I_{1x}^2 + \varepsilon_y I_{1y}^2 + \varepsilon_z I_{1z}^2) - (\varepsilon_x I_{2x}^2 + \varepsilon_y I_{2y}^2 + \varepsilon_z I_{2z}^2) \qquad (4.9)$$

$$\mathcal{H}_{HF} = \vec{S} \cdot \bar{\bar{A}} \cdot \vec{I}_1 + \vec{S} \cdot \bar{\bar{A}} \cdot \vec{I}_2 \ . \qquad (4.10)$$

For symmetry reasons the spin axes now coincide with the molecular axes x , y, z and for the same reasons as in quinoline we have assumed that the principal axes of the quadrupole interaction also are parallel to x , y and z. Moreover we expect the quadrupole splittings of the nuclear levels to be as (4.5 a,b).

The hyperfine interaction in quinoxaline has been measured

recently by Vincent (1970) in an ESR experiment. He found

$$|A_{xx}| = 21.88 \text{ MHz} \quad , \quad |A_{yy}| = 7.3 \text{ MHz} \quad , \quad |A_{zz}| \leq 1 \text{ MHz}. \quad (4.11)$$

We make the same assumption as in quinoline and approximate the hyperfine interaction by its leading term

$$\mathcal{H}_{HF} \simeq A_{xx} S_x (I_{1x} + I_{2x}) \quad . \quad (4.12)$$

In order to find the eigenfunctions of $\mathcal{H}$ one has to diagonalize a 27×27 matrix. The analysis is greatly simplified if we use the invariance of $\mathcal{H}$ under the symmetry operations of the group C_{2v} and relative to interchange of the two nuclei. Accordingly the eigenfunctions of $\mathcal{H}_{ss} + \mathcal{H}_Q$ are written in such a form that they are bases for irreducible representations of the group C_{2v} and have a definite parity under nuclear interchange,

$$T_u \tau_{kk} = T_u \chi_{1k} \chi_{2k} \qquad (u,k,\ell = x,y,z) \quad (4.13)$$

$$T_u \tau_{k\ell}^{\pm} = \frac{1}{\sqrt{2}} T_u \{\chi_{1k}\chi_{2\ell} \pm \chi_{1\ell}\chi_{2k}\} \quad .$$

If the hyperfine interaction were absent each of the electron spin levels would consist of 6 components with energies $U + \varepsilon_k + \varepsilon_\ell$, three of which are doubly degenerate. This splitting again is independent of the electron spin state and the components of the zero-field transition would all coalesce at one single frequency.

When next introducing the h.f. interaction, which is totally symmetric, we see that it only gives matrix elements between the T_z and T_y multiplets. The non-vanishing elements occur between those substates that have (a) the same total symmetry, (b) differ by an electron spin flip $T_y \longrightarrow T_z$ together with a nuclear flip $\chi_z \longrightarrow \chi_y$ or vice versa. By arranging the spin functions symmetrywise the 27×27 interaction matrix blocks out into nine 1×1 matrices of the T_x multiplet and further into the matrices shown in table 4.2.

The spin functions with total symmetry A_1 and B_2 form 2×2 matrices. The eigenfunctions to first order and the energies to second

order are given in table 4.3. For the functions with total symmetry A_2 and B_1 the situation is slightly different. Here two 3 x 3 matrices occur, which because of near degeneracies cannot be solved by simple perturbation theory. Therefore we have diagonalized these two matrices numerically assuming $\varepsilon_z - \varepsilon_y = 3.0$ MHz , $|A_{xx}| = 21.88$ MHz and $Z - Y = 1187$ MHz. The resulting eigenfunctions together with their energies are given in table 4.3.

Inspection of the table shows the influence of hyperfine interaction again to be twofold:

(a) The nine components of the $Z - Y$ and $Z - X$ transitions will be split by the second order energy shift. As a result in the $Z - Y$ transition four components will occur with intensity ratios 2:4:2:1 and in the $Z - X$ transition five components with intensity ratios 2:4:1:1:1 .

These splittings are observed in the spectra of quinoxaline-d_6 (fig. 4.5). The allowed $Z - Y$ line at 1210 MHz at low power is indeed split into 4 components with separations and relative intensities very close to the predicted values. In the $Z - X$ transition, where the second order energy splitting is half as small, this splitting is not resolved, but the shape of the line at low power is very close to the predicted one. From the separation of the components in the "allowed" $Z - Y$ line we calculate $|A_{xx}| = 21.1$ MHz which is very close to the value $|A_{xx}| = 21.88$ MHz found by Vincent (1970) in an ESR experiment.

(b) Forbidden lines will occur. In the $Z - X$ transition two sets of four lines displaced by about $\pm(\varepsilon_y - \varepsilon_z) = \pm 3$ MHz and with relative transition probabilities of about 10^{-3} , which correspond with one nuclear flip in addition to an electron spin transition should occur. However additional forbidden lines are expected: in both the $Z - X$ and $Z - Y$ transitions two lines displaced by $\pm 2(\varepsilon_y - \varepsilon_z) \simeq 6$ MHz with relative transition probabilities of about 2×10^{-2} . These lines correspond with two nuclear spin flips in addition to the electron spin transition. They are related to the spin function $T_z\tau_{yy}$, $T_z\tau_{zz}$ of block A_2 and $T_y\tau_{yy}$, $T_y\tau_{zz}$ of B_1 , which are mixed with each other.

Table 4.2

	$T_z\tau_{xx}$	$T_z\tau_{yy}$	$T_z\tau_{zz}$	$T_y\tau^{+}_{yz}$	$T_y\tau^{-}_{yz}$
$T_z\tau_{xx}$	$Z + 2\varepsilon_x$				
$T_z\tau_{yy}$		$Z + 2\varepsilon_y$		$A_{xx}\sqrt{2}$	
$T_z\tau_{zz}$			$Z + 2\varepsilon_z$	$-A_{xx}\sqrt{2}$	
$T_y\tau^{+}_{yz}$		$A_{xx}\sqrt{2}$	$-A_{xx}\sqrt{2}$	$Y + \varepsilon_y + \varepsilon_z$	
$T_y\tau^{-}_{yz}$					$Y + \varepsilon_y + \varepsilon_z$

(a) A_2 basis

	$T_y\tau_{xx}$	$T_y\tau_{yy}$	$T_y\tau_{zz}$	$T_z\tau^{+}_{yz}$	$T_y\tau^{-}_{yz}$
$T_y\tau_{xx}$	$Y + 2\varepsilon_x$				
$T_y\tau_{yy}$		$Y + 2\varepsilon_y$		$-A_{xx}\sqrt{2}$	
$T_y\tau_{zz}$			$Y + 2\varepsilon_z$	$A_{xx}\sqrt{2}$	
$T_z\tau^{+}_{yz}$		$-A_{xx}\sqrt{2}$	$A_{xx}\sqrt{2}$	$Z + \varepsilon_y + \varepsilon_z$	
$T_z\tau^{-}_{yz}$					$Z + \varepsilon_y + \varepsilon_z$

(b) B_1 basis

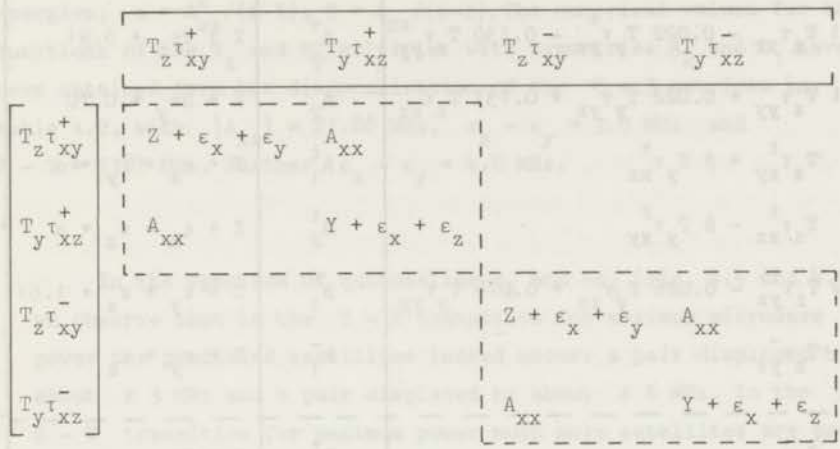

(c) A_1 basis

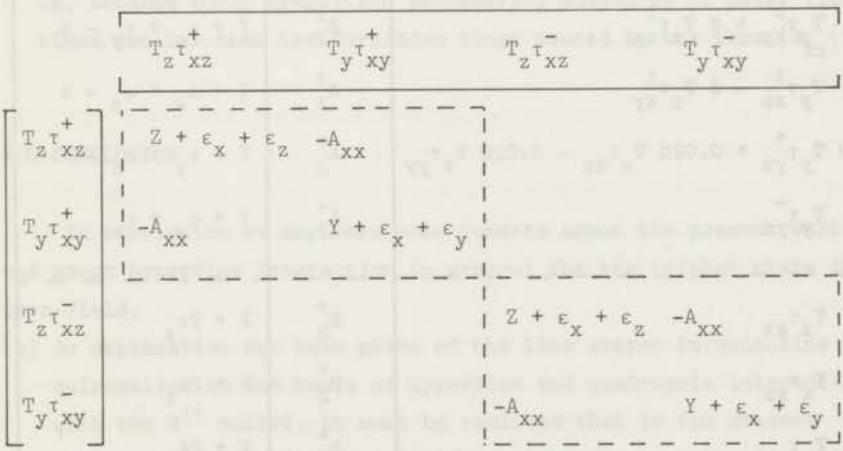

(d) B_2 basis

Table 4.2

The hamiltonian matrix for quinoxaline blocked out symmetrywise. The spin states of the T_x multiplet which do not yield any off-diagonal elements are not given.

Table 4.3

Spin eigen functions	Symmetries	Energies in MHz
$T_z\tau_{xx}$	A_2^+	$Z + 2\varepsilon_x$
$0.991\ T_z\tau_{zz} - 0.022\ T_y\tau^+_{yz} - 0.130\ T_z\tau_{yy}$	A_2^+	$Z + 2\varepsilon_z + 0.91$
$0.991\ T_z\tau_{yy} + 0.022\ T_y\tau^+_{yz} + 0.131\ T_z\tau_{zz}$	A_2^+	$Z + 2\varepsilon_y + 0.70$
$T_z\tau^\pm_{xy} + \beta\ T_y\tau^\pm_{xz}$	$A_1^\pm$	$Z + \varepsilon_x + \varepsilon_y + \alpha$
$T_z\tau^\pm_{xz} - \beta\ T_y\tau^\pm_{xy}$	$B_2^\pm$	$Z + \varepsilon_x + \varepsilon_z + \alpha$
$0.999\ T_z\tau^+_{yz} - 0.026\ T_y\tau_{zz} + 0.026\ T_y\tau_{yy}$	B_1^+	$Z + \varepsilon_y + \varepsilon_z + 1.61$
$T_z\tau^-_{yz}$	B_1^-	$Z + \varepsilon_y + \varepsilon_z$
$T_y\tau_{xx}$	B_1^+	$Y + 2\varepsilon_x$
$0.991\ T_y\tau_{zz} + 0.022\ T_z\tau^+_{yz} + 0.131\ T_y\tau_{yy}$	B_1^+	$Y + 2\varepsilon_z - 0.70$
$0.991\ T_y\tau_{yy} - 0.022\ T_z\tau^+_{yz} - 0.130\ T_y\tau_{zz}$	B_1^+	$Y + 2\varepsilon_y - 0.91$
$T_y\tau^\pm_{xy} + \beta\ T_z\tau^\pm_{xz}$	$B_2^\pm$	$Y + \varepsilon_x + \varepsilon_y - \alpha$
$T_y\tau^\pm_{xz} - \beta\ T_z\tau^\pm_{xy}$	$A_1^\pm$	$Y + \varepsilon_x + \varepsilon_z - \alpha$
$0.999\ T_y\tau^+_{yz} + 0.026\ T_z\tau_{zz} - 0.026\ T_z\tau_{yy}$	A_2^+	$Y + \varepsilon_y + \varepsilon_z - 1.61$
$T_y\tau^-_{yz}$	A_2^-	$Y + \varepsilon_y + \varepsilon_z$
$T_x\tau_{xx}$	B_2^+	$X + 2\varepsilon_x$
$T_x\tau_{zz}$	B_2^+	$X + 2\varepsilon_z$
$T_x\tau_{yy}$	B_2^+	$X + 2\varepsilon_y$
$T_x\tau^\pm_{xy}$	$B_1^\pm$	$X + \varepsilon_x + \varepsilon_y$
$T_x\tau^\pm_{xz}$	$A_2^\pm$	$X + \varepsilon_x + \varepsilon_z$
$T_x\tau^\pm_{yz}$	$A_1^\pm$	$X + \varepsilon_y + \varepsilon_z$

Table 4.3

Approximate spin functions for quinoxaline and corresponding eigenenergies; $\alpha = A_{xx}^2/(Z-Y)$, $\beta = A_{xx}/(Z-Y)$. The numerical values for the functions of the T_z and T_y multiplet with symmetries A_2 and B_1 have been obtained from the diagonalization of the 3 x 3 matrices in table 4.2, with $|A_{xx}| = 21.88$ MHz, $\epsilon_z - \epsilon_y = 3.0$ MHz and $Z - Y = 1187$ MHz. Further $\epsilon_x - \epsilon_y = 4.0$ MHz.

In the spectrum of quinoxaline-h_6 and $-d_6$ (fig. 4.4 and 4.5) we observe that in the Z - X transition for maximum microwave power the predicted satellites indeed occur: a pair displaced by about ± 3 MHz and a pair displaced by about ± 6 MHz. In the Z - Y transition for maximum power much more satellites are present than the two predicted by the model. Quite a number of mechanisms may be responsible for these additional lines. They might arise through the neglected terms in the hyperfine interaction $|A_{yy}|$ and $|A_{zz}|$. However, it is surprising that such lines would show up, because their transition probability should be at least 100 times smaller than the forbidden lines caused by the term $|A_{xx}|$.

4.4 CONCLUSION

In conclusion we may make some remarks about the present work and about hyperfine interaction in general for the triplet state in zero-field.

(a) An explanation has been given of the line shapes in quinoline and quinoxaline on the basis of hyperfine and quadrupole interaction with the N^{14} nuclei. It must be realized that in the present instance the solution is relatively simple because the term $|A_{xx}|$ of the h.f. interaction with the N^{14} nuclei is the most important. In general there is not such a large difference between the h.f. terms and many additional forbidden transitions may occur. As a result the line shapes may become very complicated and make it necessary to use numerical methods to find the theoretical shape.

(b) Although it was indicated in section 2.1 that groups of protons may contribute to the line width of the zero-field transitions we have neglected them in the present analysis. Here we shall estimate their effect on the line width in the aza-aromatics by looking at the hyperfine interaction with two equivalent protons.

In naphthalene as well as in quinoline and quinoxaline (Hirota et al. 1964, Vincent and Maki 1963, 1965) h.f. interaction with the α protons is considerably larger than with the β protons and we neglect the effect of the latter. Two equivalent α protons with $I = \frac{1}{2}$ may be combined to nuclear states having $I = 0$ and $I = 1$. Hyperfine interaction with the nuclear singlet state vanishes and as we know the presence of a nuclear spin $I = 1$ gives a second order splitting. In general one expects four components, with a maximum splitting of about $A_{xx}^2/(Z-Y) \approx 0.3$ MHz. The total effect of all protons of course will be slightly larger and a linebroadening in the order of 0.5 - 1 MHz can be expected. An exact calculation on naphthalene-h_8 has been performed by Hutchison, Nicholas and Scott (1970). They predict structureless zero-field spectra with linewidths of 1 - 1.4 MHz and confirm this prediction with spectra observed in a microwave zero-field spectrometer.

The contributions to the linewidths of the protons in the two aza-aromatic molecules may be expected to be about the same as the second order splittings due to the N^{14} nucleus. Hence in quinoline-h_7 and quinoxaline-h_6 the "forbidden" lines are still separated from the "allowed" ones, but the structure in the "allowed" part is lost.

(c) Recently Buckley and Harris (1970) have observed beautifully resolved zero-field spectra of 2,3-dichloroquinoxaline where forbidden lines occur involving a simultaneous nuclear Cl^{35} or Cl^{37} transition. The quadrupole splittings of these nuclei are about 35 MHz and the "forbidden" lines are very well separated from the "allowed" ones. In more recent work Fayer, Harris and Yuen (1970) even observed satellites involving nuclear Cl^{35} and Cl^{37} transitions of neighbouring "host" molecules.

From the experimental material presently available it may be

concluded that zero-field spectroscopy offers a tool for measuring the quadrupole splittings of nitrogen and chlorine nuclei of molecules in their phosphorescent triplet state.

(d) It has been shown by Chan et al. (1969) in this laboratory and by Harris et al. (1969) that it is possible to do ENDOR experiments on photo-excited triplets in zero-field. The experimental set-up is analogous to that described in section 3.1 with the addition of an r.f. oscillator for saturating the nuclear transitions, which is connected to the microwave helix or to a second coil surrounding the sample. In this way the transitons between the nuclear levels of an electron spin multiplet are observed via a change of the phosphorescence intensity and in favorable cases the hyperfine splitting can be analyzed with much higher precision than in the present work. However the analysis in molecules containing hydrogen atoms often proves to be very complicated because of additional effects due to h.f. interaction with the protons.

CHAPTER 5

THE DYNAMICS OF POPULATING AND DEPOPULATING THE PHOSPHORESCENT STATE

5.1 INTRODUCTION

From the steady state experiments described in chapter 4 we know that at 4.2 K in naphthalene, quinoline and quinoxaline relaxation between the spin levels of the triplet state is much faster than the decay. In fact this fast relaxation allowed us to use modulation techniques for the detection of zero-field spectra at frequencies higher than the decay rates k_u.

The relaxation rates are strongly temperature dependent (de Groot et al. 1967) and we therefore investigated whether by lowering the temperature we could reach a situation where relaxation becomes slow compared to the decay rates of the individual levels. It turned out that in many molecules this situation indeed occurs (Antheunis et al. 1970). During the decay of such an "isolated" triplet system drastic changes may be induced in the phosphorescence intensity by the sudden irradiation of a microwave transition between a pair of levels (Schmidt, Veeman and van der Waals 1969). As an example we have shown in fig. 5.1 the decay of quinoline-h_7 in durene at 1.25 K. At a time t = 1.28 s after shutting off the exciting light the microwave frequency is swept through the Z - X transition at 3585 MHz and a sharp increase in light intensity occurs.

Since the first observation of such a "microwave induced delayed phosphorescence signal" we have developed it into a system of transient

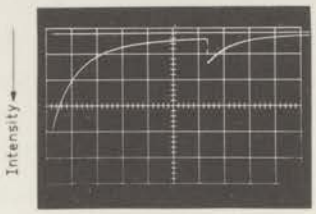

Fig. 5.1 The decay of phosphorescent quinoline-h_7 in durene at 1.25 K. Horizontal 0.2 s per division. The delayed signal is induced by sweeping through the Z - X transition at 3585 MHz, 1.28 s after shutting off the exciting light.

experiments for solving the dynamics of populating and depopulating the individual spin components of the phosphorescent triplet state. A preliminary discussion of this method has already been given with phenazine as an example (Antheunis et al. 1970). In this chapter we shall present a more complete description of the technique and illustrate it with experiments on our molecules of interest: quinoline and quinoxaline.

5.2 THE EXPERIMENTAL METHOD AND RESULTS FOR QUINOLINE-h_7 IN DURENE

In order to demonstrate the essential features of the technique we shall consider the "almost ideal" case of quinoline-h_7. The positions of the spin levels of this molecule have been indicated in fig. 5.2 together with the rate processes that govern the steady state populations of the three components.

1. The populating rates P_u of components T_u $(u = x, y, z)$.
2. The absolute rates of decay k_u from T_u to the ground state, which consist of a radiative part k_u^r and a radiationless part k_u^d.
3. The rates of spin reorientation W_{uv} $(u, v = x, y, z)$.

By reducing the pressure above the liquid helium to 0.3 mm we obtain a temperature of 1.1 K and then find in quinoline-h_7 that

$$W_{uv} << k_x , k_y , k_z \quad . \tag{5.1}$$

When this "isolation condition" holds the spin components decay independently. We shall now show how one can take advantage of this "isolation" to measure the absolute decay rates k_u , the relative radiative decay rates k_u^r , the relative steady state populations $N_u(0)$ and the relative populating rates P_u of the three spin levels.

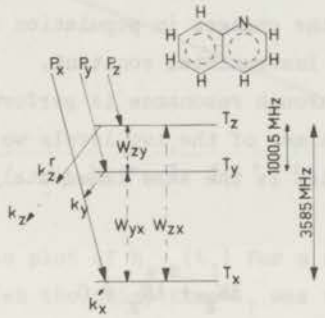

Fig. 5.2 The zero-field splitting of the lowest $\pi\pi^*$ triplet state of quinoline-h_7 in durene and the populating, depopulating and relaxation rates.

In all our examples, quinoline-h_7 and -d_7 and in quinoxaline-h_6 and -d_6 it turns out that depopulation, radiative as well as non-radiative, occurs predominantly from the top level T_z, in other words: $k_z^r >> k_y^r , k_x^r$ and also $k_z >> k_y , k_x$.

The absolute decay rates k_u .

These we measure in experiments such as that shown in fig. 5.1. The sample is irradiated at 1.1 K, where the isolation condition (5.1) holds, and a steady state population established. Then the exciting light is shut off (t = 0) and the phosphorescence monitored with a photomultiplier connected to the oscilloscope. The signal one initially

observes is almost entirely caused by the fast decay of the emitting level T_z. At a time $t = t_1$ long compared with the decay time k_z^{-1} of T_z, one suddenly sweeps the microwave field through the Z - X resonance at 3585 MHz. In this way molecules are taken from the slowly decaying non-active level T_x to repopulate the emitting level T_z and a sharp increase in phosphorescence is observed (fig. 5.1). The height $h_{x\to z}(t_1)$ of the leading edge of this delayed signal is given by :

$$h_{x\to z}(t_1) = c\,(\Delta N_z\, k_z^r + \Delta N_x\, k_x^r) \quad , \tag{5.2}$$

where ΔN_x and ΔN_z are the changes in population induced by the microwave field and c is an instrumental constant.

Since the sweep through resonance is performed in a time short compared with the lifetimes of the two levels we may assume that the total number of molecules is the same immediately before and after the sweep. Hence

$$\Delta N_z + \Delta N_x = 0 \quad . \tag{5.3}$$

The changes in population produced by the resonance may be expressed as a fraction of the population difference between T_x and T_z that existed the moment the sweep was started

$$\Delta N_z = -\Delta N_x = f\,\{N_x(t_1) - N_z(t_1)\} \quad . \tag{5.4}$$

We now write

$$h_{x\to z}(t_1) = c\,f\,\{N_x(t_1) - N_z(t_1)\}(k_z^r - k_x^r) \quad , \tag{5.5}$$

where the fraction f depends on the experimental conditions and in particular on the microwave power (see below).

The decay rate k_x is lower than k_z and hence the time t_1 can be chosen such that $N_z(t_1)$ is negligible relative to $N_x(t_1)$. If the initial steady state populations $N_z(0)$ and $N_x(0)$ are about the same the condition $t_1 \geq 5\, k_z^{-1}$ suffices. We then may approximate (5.5) by

$$h_{x\to z}(t_1) \simeq c\, f\, N_x(t_1)(k_z^r - k_x^r) \quad . \tag{5.6}$$

In fig. 5.3 $\log h_{x\to z}(t_1)$ has been plotted against t_1 . For times $t_1 \geq 2$ s the condition $N_x >> N_z$ applies and a straight line results. If relaxation is negligible the slope κ_x of this line must be equal to the rate constant k_x that we seek.

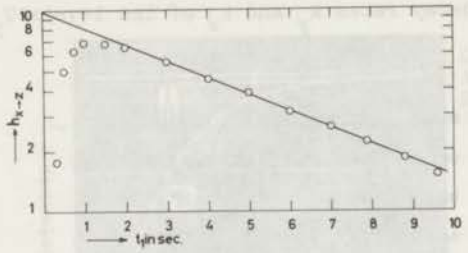

Fig. 5.3 A logarithmic plot of $h_{x\to z}(t_1)$ for a series of experiments on quinoline-h_7 in which the delay time t_1 was varied; T = 1.1 K. The slope of the straight line for $t \geq 2$ s is equal to κ_x. For $t_1 = 0$ the signal becomes negative, indicating that in equilibrium T_x is underpopulated relative to T_z (cf. table 5.1).

It may be noted that a logarithmic plot like fig. 5.3 provides a check on the assumption $N_z(t_1) \simeq 0$; for $t \leq 2$ s when this is not yet true, the line is noticeably curved. It will be clear that one can do a similar experiment with the other "dark" level T_y by sweeping through the Z - Y transition at 1000.5 MHz.

If the relaxation rates W_{uv} are not completely negligible the slowly decaying levels to some extent are kept in contact with the fast decaying level T_z. The observed slopes κ_x and κ_y then will not be equal to the absolute decay rates k_x and k_y of the individual levels as defined in fig. 5.2. In order to verify that effective isolation had been achieved we have repeated the measurements at higher temperatures. The results in fig. 5.4 show that κ_y remains constant from 1.1 to 1.25 K but that in the same temperature region κ_x already slightly

increases. At temperatures higher than 1.25 K the observed values increase rapidly with temperature because spin relaxation opens an extra decay route for the two dark levels via the fast decaying level T_z . If we assume that W_{uv} still decreases on cooling from 1.25 to 1.1 K, where the observed decay rates remain constant, it may be concluded that at 1.1 K relaxation has a small effect. Although the real temperature dependence of W_{uv} between 1.1 and 1.25 K is unknown, we assume that in the case of quinoline-h_7 at 1.1 K the observed rates are the absolute decay rates k_y and k_x of the levels T_y and T_x .

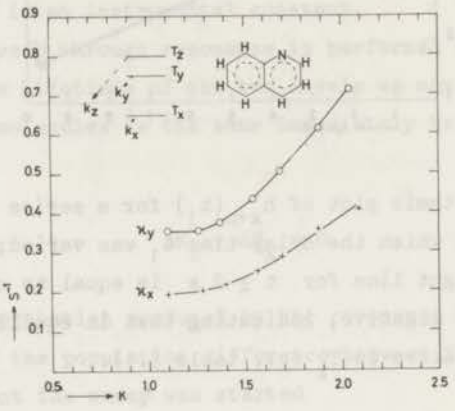

Fig. 5.4 The apparent decay rates κ_y and κ_x of quinoline-h_7 in durene as a function of temperature.

We are left with the determination of the absolute decay rate of the radiative level T_z . This problem can be solved in the following way. We remember that the delayed phosphorescence is caused by selective repopulation of T_z from a "dark" level. Hence the tail of this signal represents the decay of T_z. The base line of this decay almost coincides with the line of zero light intensity because in the present case the radiative decay rates of the "dark" levels are small and phosphorescence from impurities may be neglected. As an illustration we show in fig. 5.5 the decay of quinoline-h_7 under

different experimental conditons. All traces start 5 s after shutting off the exciting light and the time scale is 0.2 s per division. Trace A represents the delayed signal induced by a sudden sweep through the Z - X transition at 3585 MHz. Trace B is the normal decay and C the line of zero light intensity. The phosphorescence emitted by the repopulated radiative level T_z quickly decays to a value very close to zero and hence in this picture C can be used as a base line without introducing an important error.

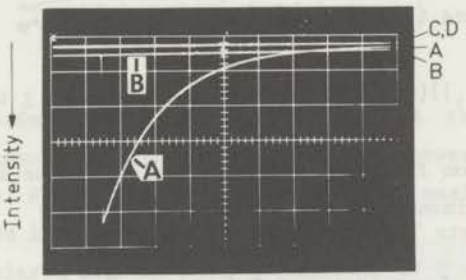

Fig. 5.5 The decay of phosphorescent quinoline-h_7 in durene at 1.1 K. The traces start 5 s after shutting off the exciting light and the time scale is 0.2 s per division. A: delayed signal induced by a sudden sweep through the Z - X transition at 3585 MHz. B: normal decay, C: zero line, D: decay when the Z - X transition is continuously saturated. In this particular experiment the trace D coincides with C and shows its presence only in the beginning as a broadening of C.

If the radiative rates of the spin levels are less extreme than in quinoline, we need the exact position of the baseline of the delayed signal for a precise measurement of the absolute decay rate of the repopulated level. In order to show how such a base line is determined we have displayed in fig. 5.5 the result of an additional experiment D, in which the Z - X transition is continuously saturated from the moment the exciting light is shut off. Via the microwave transitions the slowly decaying level T_x is kept in contact with the radiative level T_z and the two levels decay together. At the

moment trace D starts (t = 5 s) we may then assume both T_z and T_x to be empty. Hence the difference $B(t_1) - D(t_1)$ just before the microwave sweep starts is due to molecules in T_x which in B contributed to the phosphorescence via their weak radiative decay k_x^r. (In the present case where D practically coincides with C, we know moreover that phosphorescence from T_y or from impurities, at t = 5 s or longer, may be neglected.) When the delayed signal is induced at time t_1 a fraction f of $N_x(t_1)$ is transferred to the emitting level T_z and a fraction $(1 - f)N_x(t_1)$ left behind. Thus, the base line of the delayed signal is found by adding to trace D a value

$$\{B(t_1) - D(t_1)\}(1 - f) \exp\{-(t - t_1)k_x\} \qquad (t \geq t_1) \quad . \tag{5.7}$$

In this expression f is still unknown and its value is obtained from a separate experiment.

T h e t r a n s f e r c o e f f i c i e n t f .

This parameter is measured by sweeping twice through the Z - X transition. First at time t_1 generating a delayed signal with a height given by (5.6) and again at time t_2 such that $t_2 - t_1 \geq 5\, k_z^{-1}$. Hence just before the second signal is induced the radiative level T_z again is empty, while the dark level T_x carries a population

$$N_x(t_2) = (1 - f)\, N_x(t_1) \exp\{-(t_2 - t_1)k_x\} \quad . \tag{5.8}$$

The expression for the second delayed signal then becomes

$$h_{x \to z}(t_2) = c\, f\, (1 - f)\, N_x(t_1) \exp\{-(t_2 - t_1)k_x\}\, (k_z^r - k_x^r) \quad . \tag{5.9}$$

From the ratio of the heights of the two consecutive signals - (5.9) at time t_2 and (5.6) at t_1 - we find the value of f.

The results of such f measurements for the Z - X transition in quinoline-h_7 as a function of microwave power are displayed in fig. 5.6. At the maximum microwave power of 200 mW and a sweep rate of 10 MHz/ms , f reaches a value of 0.715.

It may look surprising that the transfer coefficient is higher

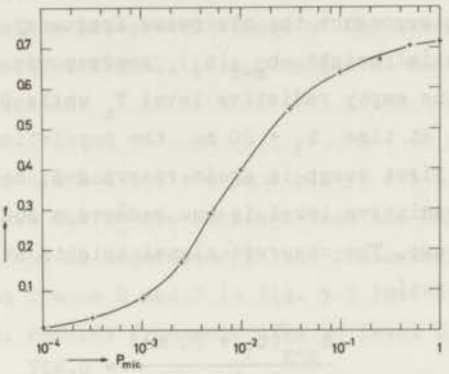

Fig. 5.6 The transfer coefficient f for the Z - X transition in quinoline-h_7 in durene as a function of microwave power; T = 1.1 K. The relative value $P_{mic} = 1$ corresponds with the maximum microwave power of 200 mW fed into the helix. The values of f are obtained from two consecutive delayed signals with an interval of 2 s induced between 5 and 10 s after shutting off the exciting light. The result f = 0.715 for maximum microwave power is the average of 5 measurements and has a standard deviation of 0.005.

than 0.5, the value corresponding with saturation of the transition. Indeed in our previous example phenazine (Antheunis et al. 1970) we found f very close to 0.5 and concluded that in this case saturation was achieved. In the mean time it has been shown by Harris (1971) that a sweep through one of the resonances of a triplet state in zero-field may lead to a partial inversion of the populations of the two spin levels. This effect is analogous to the well known adiabatic fast passage in magnetic resonance and it occurs when coherent coupling exists between the triplet system and a strong microwave magnetic field. In the next chapter we shall give a description of such coherent interaction and its effect on phosphorescence. Here we merely note that a partial inversion may indeed occur as shown by our observation that in quinoline-h_7 at maximum microwave power f = 0.715 .

A nice visual proof of this phenomenon is shown in fig. 5.7 ,

where the Z - X delayed signal is again presented, but now after the first sweep through resonance the microwave frequency is immediately swept back. The initial height $h_{X\to Z}(t_1)$ corresponds with a transfer of $0.715N_X(t_1)$ to the empty radiative level T_Z while $0.285N_X(t_1)$ is left behind in T_X. At time $t_1 + 20$ ms the population difference established by the first sweep is again rearranged; because the population of the radiative level is now reduced a sudden reduction in phosphorescence occurs. The observed signal heights at times t_1 and $t_1 + 20$ ms have a ratio:

$$\frac{h_{Z\to X}(t_1 + 20\ \text{ms})}{h_{X\to Z}(t_1)} = 0.427 \quad .$$

This is in good agreement with the theoretical value 0.413 calculated for a transfer coefficient of 0.715 in both sweeps.

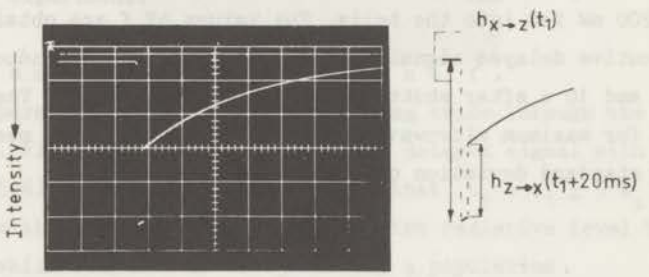

Fig. 5.7 The delayed phosphorescence signal of quinoline-h_7 in durene, induced by a sudden sweep through the Z - X transiton at 3585 MHz with the maximum microwave power of 200 mW: sweep rate 10 MHz/ms, f = 0.715, T = 1.1 K. The trace starts 5 s after shutting off the exciting light and the time scale is 0.1 s per division. The microwave frequency is swept back 20 ms after the first sweep and a sudden decrease of the delayed signal occurs. (Since the trace is difficult to follow, it is redrawn at the right.)

We preferred to induce the delayed signals by sweeping through resonance in stead of applying a monochromatic microwave pulse. In this way we affect the whole spectrum and not only a slice of the inhomogeneously broadened zero-field lines. We must not forget however

that very different transition probabilities occur in the spectrum (chapter 4). Hence the integrated effect of the sweep through resonance, measured as the delayed signal, is a complicated mixture of saturation and adiabatic inversion.

R e l a t i v e r a d i a t i v e d e c a y r a t e s k_u^r .

Once f is known the k_u^r are obtained from the experiment displayed in fig. 5.5. This can be understood in the following way. The difference between traces B and D in fig. 5.5 just before the delayed signal is induced, results from molecules in level T_x :

$$B(t_1) - D(t_1) = c\, N_x(t_1) k_x^r \quad , \tag{5.10}$$

while the height of the delayed signal is given by (5.6). From the two expressions and the value of f we deduce the ratio of k_x^r and k_z^r. The ratio of k_z^r and k_y^r can be determined in an analogous manner. The results summarized in table 5.1 refer to experiments at 1.1 K and show that indeed the top level T_z is by far the most radiative.

T h e r e l a t i v e s t e a d y s t a t e p o p u l a t i o n s $N_u(0)$ can now be found as follows. The phosphorescence at $t = 0$ is given by

$$I(0) = c \sum_u N_u(0)\, k_u^r \quad . \tag{5.11}$$

Further, for the height of the delayed signal $h_{x\to z}(t_1)$ for sufficiently long t_1 we have the expression (5.6). This may also be written as

$$h_{x\to z}(t_1) = c\, f\, N_x(0)\, \exp\{-k_x t_1\}(k_z^r - k_x^r) \quad . \tag{5.12}$$

One has a similar expression to refer $h_{y\to z}(t_1)$ to the steady state value $N_y(0)$. From these two equations together with (5.11) we find $N_x(0) : N_y(0) : N_z(0)$, because the values of f , k_u and k_u^r are known.

Table 5.1

	quinoline-h_7 in durene	σ	quinoxaline-h_6 in naphthalene-d_8	σ	naphthalene-h_8 in naphthalene-d_8
k_z	3.1 s^{-1}	0.03 s^{-1}	12.0 s^{-1}	0.2 s^{-1}	0.65 s^{-1}
k_y	0.32 s^{-1}	0.02 s^{-1}	0.80 s^{-1}	0.02 s^{-1}	0.40 s^{-1}
k_x	0.19 s^{-1}	0.01 s^{-1}	0.42 s^{-1}	0.01 s^{-1}	0.15 s^{-1}
k_z^r	1		1		
k_y^r	0.036	0.008	0.013	0.002	
k_x^r	0.025	0.002	0.013	0.001	
$N_z(0)$	1		1		
$N_y(0)$	0.194	0.023	0.362	0.034	
$N_x(0)$	0.554	0.037	0.362	0.015	
P_z	1		1		
P_y	0.020	0.003	0.024	0.003	
P_x	0.034	0.003	0.013	0.001	
P_z^f	1		1		
P_y^f	0.024	0.003	0.032	0.003	
P_x^f	0.033	0.002	0.021	0.001	

Table 5.1

Decay rates k_u in s^{-1}, relative radiative decay rates k_u^r, relative steady state populations $N_u(0)$ and relative populating rates P_u of the spin components of the phosphorescent triplet states of quinoline-h_7 in durene and quinoxaline-h_6 in naphthalene-d_8 as measured at 1.1 K. At this temperature isolation is obtained in both systems and the values given are believed to represent the properties of the individual spin levels. The decay rates in the last column for naphthalene were obtained from ESR experiments by Schwoerer and Sixl (1968, 1969) at 4.2 K. The results in the bottom section refer to flash experiments; all others to experiments in which a steady state was first established. All values are averages of three measurements performed on two different samples, cut from one large single crystal. The symbol σ stands for the standard deviation of the mean.

The relative populating rates P_u.
These follow by combining the decay rates with the steady state populations of the levels. Because, when relaxation may be neglected the change of population per unit time of level T_u is determined by

$$\frac{dN_u}{dt} = P_u - N_u k_u \quad , \quad (u = x, y, z) \quad . \tag{5.13}$$

In steady state the change of population per unit time is zero and hence

$$N_u(0) = \frac{P_u}{k_u} \quad . \tag{5.14}$$

Since N_u and k_u are known we find the relative populating rates P_u given in table 5.1.

As a check on the steady state experiments we have measured P_u also in flash experiments. It follows from (5.13) that immediately after an excitation by a flash of duration $\tau \ll k_u^{-1}$ the populations of the spin components are proportional to their populating rates P_u. These "flash" populations were determined in the same way as in the steady state experiments. The results of this method are also given in

table 5.1 and it is satisfying to find that there is close agreement between the two methods.

5.3 FURTHER RESULTS

In addition to quinoline-h_7 we have applied the same method to the systems quinoline-d_7 in durene, quinoxaline-h_6 and -d_6 in durene and quinoxaline in naphthalene-d_8. The experimental method for measuring the dynamics is the same as for quinoline-h_7 and needs no further comment. We shall now consider the different systems.

Q u i n o l i n e - d_7 i n d u r e n e . (table 5.2)

In this molecule the absolute decay rates k_u are lower than in quinoline-h_7 because by deuteration of the molecule the nonradiative decay rates k_u^d are decreased. It is not possible to obtain good isolation as can be seen in fig. 5.8. The values κ_y and κ_x derived from the experiments do not become independent of temperature in the temperature range covered. As a result, the values κ_u , k_u^r , $N_u(0)$ and

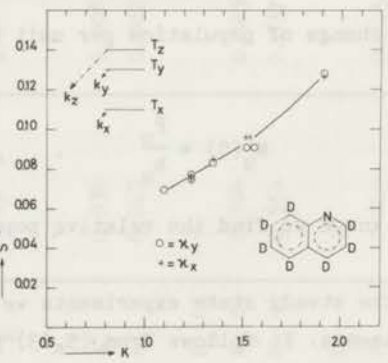

Fig. 5.8 The apparent decay rates κ_y and κ_x of quinoline-d_7 in durene as a function of temperature.

P_u for T_y and T_x do not represent the properties of the isolated levels. For example we expect the true k_y and k_x to be lower than the measured $\kappa_y = 0.069$ and $\kappa_x = 0.068\ s^{-1}$. However the top level T_z decays much faster and κ_z must be very close to the value k_z. We have only given σ, the standard deviation of the mean for the measurements of κ_z, because the systematic error in the other results is undoubtly larger than the variation in the measurements. Although relaxation still plays a role at 1.1 K we observe that the steady state populations deviate from a Boltzmann distribution because the top level T_z with its fast decay to a large extent is independent of the other two.

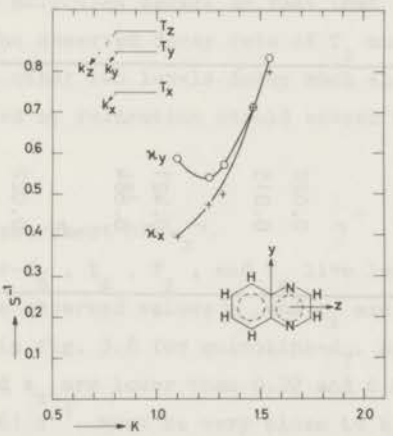

Fig. 5.9 The apparent decay rates κ_y and κ_x of quinoxaline-h_6 in durene as a function of temperature.

Quinoxaline-h_6 and -d_6 in durene. (table 5.2)

In quinoxaline-h_6 the values κ_y and κ_x differ at 1.1 K (fig. 5.9) but we do not find a temperature independent behaviour. The properties of T_y and T_x are again affected by relaxation. We expect that k_y is slightly higher than $0.59\ s^{-1}$ and k_x slightly lower than $0.40\ s^{-1}$. The value $\kappa_z = 11.1\ s^{-1}$ however must be very close to k_z. We have only

Table 5.2

	quinoline-d_7 in durene	σ	quinoxaline-h_6 in durene	σ	quinoxaline-d_6 in durene	σ
κ_z	1.05 s^{-1}	0.03 s^{-1}	11.1 s^{-1}	0.2 s^{-1}	6.61 s^{-1}	0.1 s^{-1}
κ_y	0.069 s^{-1}		0.59 s^{-1}		0.22 s^{-1}	
κ_x	0.068 s^{-1}		0.40 s^{-1}		0.20 s^{-1}	
k_z^r	1		1		1	
k_y^r	0.028		0.020		0.020	
k_x^r	0.043		0.015		0.038	
$N_z(0)$	1		1		1	
$N_y(0)$	0.676		0.421		0.742	
$N_x(0)$	1.028		0.684		0.788	
P_z	1		1		1	
P_y	0.044		0.022		0.025	
P_x	0.067		0.025		0.024	
P_z^f	1		1		1	
P_y^f	0.047		0.019		0.024	
P_x^f	0.027		0.025		0.023	

Table 5.2

Apparent decay rates κ_u in s^{-1}, relative radiative decay rates k_u^r, relative steady state populations $N_u(0)$ and relative populating rates P_u of the spin components of the phosphorescent triplet states of quinoline-d_7 and quinoxaline-h_6 and -d_6 in durene. Except for quinoxaline-d_6 where we worked at 1.24 K the numbers refer to experiments at 1.1 K. The results in the bottom section again refer to flash experiments; the others to experiments in which a steady state was first established. All values are averages of three measurements performed on two different samples cut from one large single crystal. In neither of the three systems complete isolation is obtained and the values for T_y and T_x do not correspond exactly with the properties of the individual spin levels because relaxation cannot be neglected. We have only given the value of σ for the measurements of κ_z. The top level of the three molecules decays so fast that it hardly "feels" the other levels and the observed decay rate of T_z must be close to the real value k_z. The other two levels decay much slower and the systematic error introduced by relaxation should exceed the value of σ.

given σ for the measurement of κ_z.

In quinoxaline-d_6, T_x, T_y, and T_z live longer than in quinoxaline-h_6. The observed values κ_y and κ_x are equal and temperature dependent just as in fig. 5.8 for quinoline-d_7. Again no isolation is obtained and k_y and k_x are lower than 0.22 and 0.20 s^{-1} respectively. The value $\kappa_z = 6.61\ s^{-1}$ must be very close to k_z. Again σ is only given for the measurement of κ_z.

Our results for κ_z in quinoxaline-h_6 and -d_6 are identical to the values obtained by de Groot et al. (1969). It has been remarked by these authors that the decay rates of quinoxaline-h_6 and -d_6 at 4.2 K increased with about 5% over a period of about a year. Our results are obtained on new "fresh" crystals, but in the old crystals formerly used by them we found κ_z to be about 4% higher. However the apparent decay rates for the other two levels and also their temperature dependence turned out to be the same. Apparently this "aging" only affects the radiative level T_z. The reason for this effect may perhaps be the diffusion of oxygen into the crystal, as suggested by the former

authors.

Quinoxaline-h_6 in naphthalene-d_8.(table 5.1)

In order to check the influence of the matrix and see if we could attain better isolation we have also measured the dynamics for quinoxaline-h_6 present as a substitutional guest in a single crystal of naphthalene-d_8. In this crystal the quinoxaline triplet state forms a shallow trap and phosphorescence is only observed at helium temperatures (Hammer et al. 1970). We were fortunate to find that, contrary to the system quinoxaline-durene, κ_y and κ_x become temperature independent below 1.5 K (see fig. 5.10). This suggests that in this crystal isolation obtains at 1.1 K. Hence the values given in table 5.1 represent the properties for the isolated sublevels. We indeed find that they are more extreme than in the system quinoxaline-durene.

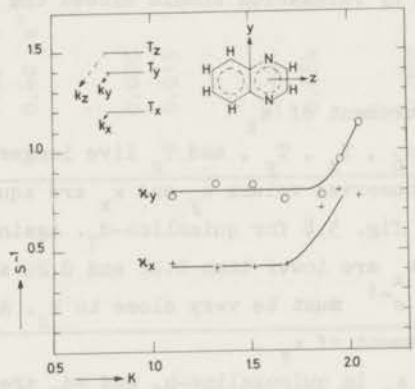

Fig. 5.10 The apparent decay rates κ_y and κ_x of quinoxaline-h_6 in naphthalene-d_8 as a function of temperature.

The results for the two "isolated" systems, quinoline-h_7 in durene and quinoxaline-h_6 in naphthalene-d_8 , have been given in table 5.1, while the results for the other molecules, which are known to be

affected by relaxation, are found in table 5.2. We have added values for k_u of naphthalene-h_8 obtained by Schwoerer and Sixl (1968, 1969) from ESR experiments in high field.

In order to check the effect of the matrix on the populating mechanism of the triplet state we have repeated the measurements for the durene systems with a durene solution filter in the exciting light path. In this way we ensure that only the guest singlet system is excited and prevent the host from contributing in the populating process. We did not find a substantial variation in the numbers of table 5.1 and 5.2 and concluded that with our light source the populating mechanism of the triplet state of the guest in the durene matrix is mainly an intramolecular process.

A discussion of the experimental numbers in terms of molecular properties is beyond the scope of this thesis; a preliminary analysis has already been given elsewhere (Schmidt et al. 1969). We are presently engaged in a more complete interpretation based on results for a larger group of molecules.

5.4 CONCLUSION

Using quinoline and quinoxaline as examples we have shown that the phenomenon called "microwave induced delayed phosphorescence" can be developed into a successful technique for solving the dynamics of populating and depopulating the phosphorescent triplet state. At this point it may be useful to make some remarks about the application of the method in general.

(a) The examples given allow of a simple interpretation of the observed signals since one level dominates in the radiation and the total decay rates are very different. However, one is by no means restricted to such simple systems. Generally speaking the method is applicable if the triplet state has at least one slowly decaying spin component. In the decay of such a triplet we can always find a delay time where this "slow" level is the only one populated. With the resonant microwave field we can then repopulate each of the "fast" levels separately and measure its

properties independently of the other ones. The behaviour of the "slow" level then follows from the variation in height with the delay time. This method has been used for example in iso-quinoline (Schmidt et al. 1969) where two radiative, fast decaying levels are present which in a normal decay cannot be distinguished from each other. The same technique has been applied to pyrimidine (Burland et al. 1971) and tetra-methylpyrazine where also two "fast" radiative levels occur.

In systems with smaller differences in absolute and radiative decay rates the situation is more complex. Nevertheless, with microwave fields resonant with the three zero-field transitions, one can rearrange the populations in a variety of ways. In doing so one can generate a system of equations from which the properties of the triplet state are found.

(b) Most important is the isolation of the levels. One may expect - and this is confirmed by our experiments on phenazine (Antheunis et al. 1970) - that this condition is the easier fulfilled the higher the decay rates k_u of the triplet. Guided by the experimental material presently available we have the impression that in triplets with $k_u \leq 0.1\ s^{-1}$ it is impossible to have isolation at a temperature of 1.1 K, our experimental limit.

(c) The depopulation of the slow levels T_y and T_x at higher temperatures is affected by relaxation. For instance, in quinoline-h_7 in durene (fig. 5.4) the apparent decay rate κ_y increases faster than κ_x with increasing temperature. This indicates that W_{yz} starts to increase sooner than the other relaxation rates. Further, in quinoxaline-h_6 in durene (fig. 5.9) we see that the κ_y and κ_x first equalize and then increase with increasing temperature. Hence contrary to quinoline-h_7 the three relaxation rates seem to increase more evenly. Finally in quinoxaline-h_6 in naphthalene-d_8 at 1.1 K the relaxation rates are lower than in quinoxaline-h_6 in durene. This observation seems to indicate that part of the mechanism responsible for relaxation is due to interactions with neighbouring molecules.

So far very little is known about relaxation in phosphorescent triplet states. In the systems where isolation is obtained, the

absolute decay rates k_u are known very precisely and hence it must be possible to measure the relaxation rates by observing the increase of κ_y and κ_x with temperature. It is our purpose to study the relaxation more systematically and in doing so we hope to provide information about the origin of these processes.

CHAPTER 6

COHERENT INTERACTION WITH STRONG MICROWAVE FIELDS

6.1 INTRODUCTION

In the preceding chapter we have shown that a sweep through resonance at sufficient microwave power may lead to a partial inversion of the populations of two spin levels. This effect was first observed by Harris (1971) and he has given a theoretical discussion of the phosphorescence modulation that might arise through the coupling of a triplet state with a microwave field. The analogue of this effect is well-known in ESR and NMR, where a fast passage through resonance may lead to an inversion of the magnetization if the amplitude of the applied r.f. field exceeds the spin packet linewidth and the sweep rate moreover fulfils certain conditions (Abragam, 1961, Ch. II, XII).

In the following we shall see that the behaviour of a triplet state in zero-field can be described in the same way as a gyromagnet in a magnetic field. From this analogy one would expect that inversion might also be achieved via a so-called 180° pulse of a strong monochromatic microwave field resonant with the zero-field transition. Just as in NMR a prerequisite for such an experiment to succeed is that the r.f. magnetic field is practically constant in amplitude and direction relative to all molecules in the sample. Further, the amplitude must be such that the duration of the pulse is short relative to the time with which the different spin packets of the line get out of phase (i.e. short relative to the inverse of the width of the resonance expressed as an angular frequency).

With the microwave oscillators available to us these rather exacting conditions needed the replacement of the helix in our spectrometer by a specially constructed cavity and the selection of a system with a narrow resonance line. In this way we were able to observe a modulation of the phosphorescence of quinoline-d_7 which we attribute to the coherent coupling of its triplet state to the microwaves. In particular we have observed the inversion of the populations of the two levels by a 180° pulse.

We first consider the experiment and then discuss it in terms of the elegant geometrical model developed by Feynman, Vernon and Hellwarth (FVH, 1957) for visualizing coherent coupling of a pair of states to a radiation field. It will appear that our results hold a promise for the realization of electron spin-echo experiments on photo excited triplets in zero-field.

6.2 THE EXPERIMENT

In quinoxaline-d_7 in durene-d_{14} the Z - X transition is found at 3597 MHz and the Z - Y transition at 1001.0 MHz. We have observed the coherent modulation of phosphorescence produced by a microwave field tuned to the 1001.0 MHz major hyperfine component of the Z - Y transition (see insert fig. 6.2).

In order to obtain sufficiently strong microwave fields we constructed a tunable re-entrant cavity of a type described by Erickson (1966). This instrument replaces the helix in the experimental arrangement of fig. 3.1. The dimensions of the cylindrical cavity, as presented in fig. 6.1, were calculated from design curves given by Moreno (1948). We have indicated in fig. 6.1 b the approximate electric and magnetic field configurations. The electric field is concentrated in the narrow gap and the magnetic field in the coaxial region. By changing the position of the plunger the resonance frequency can be varied from 800 - 2200 MHz with a Q between 500 and 1000, depending somewhat on frequency and temperature.

In the experiment the cavity is immersed in liquid helium. The crystal, mounted against the light pipe, is irradiated through a hole in

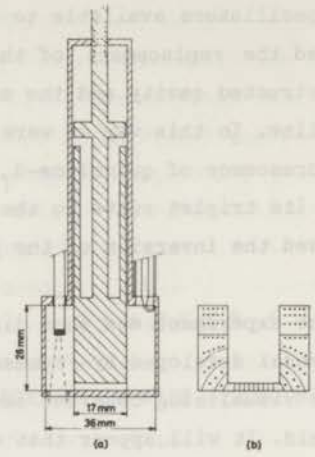

Fig. 6.1 a The tunable microwave cavity.
Fig. 6.1 b A schematic drawing of the electric and magnetic field configurations. The electric fields are indicated by the lines and the circumferential magnetic fields by dots.

the bottom of the cavity. The phosphorescence intensity is detected with the photomultiplier connected directly to the oscilloscope. The cavity is connected to a Rohde and Schwarz power signal generator with an output of 1 W via a special HP 8714 A PIN diode modulator. With this assembly microwave pulses can be generated with a duration variable between 0.1 - 100 μs. The maximum amplitude of the microwave magnetic field in the cavity then is about 1 Gauss.

The modulation of the phosphorescence is observed in the following way. The triplet state is populated by u.v. excitation at 1.1 K where relaxation is slow. (The decay rate of T_z is fast as compared with the relaxation, but T_y and T_x are not completely isolated.) When a steady state has been established the light is shut off. After $t_1 = 8$ s a delayed phosphorescence signal is induced by a 1001.0 MHz microwave pulse resonant with the Z - Y transition. From the numbers in table 5.2 we see that again the situation is such that at the moment the pulse starts T_z is empty while T_y still carries a considerable population $N_y(t_1)$. In good approximation the height of the

signal on the oscilloscope is due to the fraction $f\, N_y(t_1)$ transferred to T_z and is given by an expression similar to (5.6)

$$h_{y\to z}(t_1) \simeq c\, f\, N_y(t_1)(k_z^r - k_y^r) \qquad , \qquad (6.1)$$

where f is now a function of the microwave pulse length $\hat{t}$. The experiment is repeated with the duration of the microwave pulse as a variable. In fig. 6.2 the observed signal heights $h_{y\to z}(t_1)$ are plotted as a function of the microwave pulse duration $\hat{t}$. We observe that the signal first increases and then decreases after going through a maximum at $\hat{t}$= 0.27 μs.

If the experiment were described by means of a time-independent transition probability, one would expect the population of the radiative level T_z to increase asymptotically to a saturation value with increasing duration of the resonant field. The observed oscillatory behaviour predicted by Harris (1971) is a manifestation of

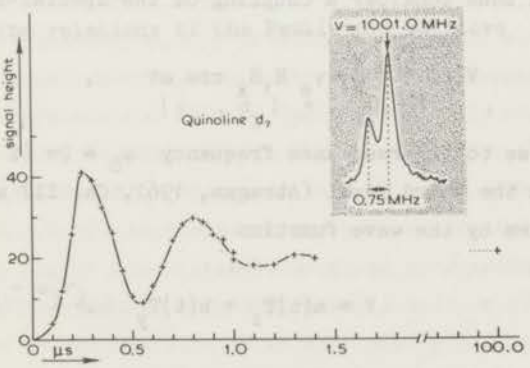

Fig. 6.2 The height of the signal $h_{y\to z}(t_1)$ induced by a microwave pulse at 1001.0 MHz, given 8 s after switching off the exciting light. The curve represents a series of experiments with varying pulse length $\hat{t}$; T = 1.1 K.

the coherence forced on the system by the microwave field. In particular we shall show that the maximum at 0.27 μs is caused by an inversion of the populations, equivalent to what in NMR is commonly called a 180° pulse.

6.3 APPLICATION OF THE FEYNMAN, VERNON AND HELLWARTH MODEL TO A PHOSPHORESCENT TRIPLET SYSTEM

We express energy again in MHz and write the Hamiltonian of the triplet system in zero-field under the influence of a radio-frequency perturbation as

$$\mathcal{H} = \mathcal{H}_{ss} + V(t) \quad , \tag{6.2}$$

where $\mathcal{H}_{ss}$ is the familiar zero-field splitting Hamiltonian. The coupling between the electron spin system and the microwave magnetic field is represented by the second term. We concentrate on the Z - Y transition and thus consider a coupling of the special form

$$V(t) = -\frac{1}{2\pi} \gamma_e H_1 S_x \cos \omega t \quad , \tag{6.3}$$

where ω is close to the resonance frequency $\omega_0 = 2\pi$ (Z - Y). We may then disregard the third level (Abragam, 1961, Ch. II) and describe our two level system by the wave function

$$\Psi = a(t)T_z + b(t)T_y \quad . \tag{6.4}$$

We are interested in the behaviour of the triplet system in time intervals short compared with the lifetimes of the spinlevels and hence assume Ψ to be normalized; $aa^* + bb^* = 1$.

The change in time of our ensemble of two level systems is given by the equation of motion of the density matrix

$$\frac{d\rho}{dt} = 2\pi i \, [\rho, \mathcal{H}] \quad . \tag{6.5}$$

The 2×2 matrices ρ and H can be written as linear combinations of the unit matrix E and the Pauli spin matrices σ_x, σ_y and σ_z,

$$\rho = \tfrac{1}{2} r_4 E + \tfrac{1}{2}(r_1\sigma_x + r_2\sigma_y + r_3\sigma_z) \quad \text{and} \tag{6.6}$$

$$\mathcal{H} = \tfrac{1}{2} \omega_4 E + \tfrac{1}{2}(\omega_1\sigma_x + \omega_2\sigma_y + \omega_3\sigma_z) \quad . \tag{6.7}$$

Since the matrices ρ and H are hermitian the coefficients in the expansions (6.6) and (6.7) are real. One finds that

$$\begin{aligned} r_1 &= \overline{ab^* + a^*b} & \omega_1 &= (V_{zy} + V_{yz}) = 0 \\ r_2 &= \overline{i(ab^* - a^*b)} & \omega_2 &= i(V_{zy} - V_{yz}) = 2\gamma_e H_1 \cos \omega t \\ r_3 &= \overline{aa^* - bb^*} & \omega_3 &= 2\pi(Z - Y) = \omega_0 \\ r_4 &= \overline{aa^* + bb^*} = 1 & \omega_4 &= 2\pi(Z + Y) = 0 \quad , \end{aligned} \tag{6.8, 6.9}$$

where $\frac{Z+Y}{2}$ (the mean energy of the levels Z and Y) has been taken as the zero of energy.

One finds by substituting (6.6) and (6.7) into (6.5), and because of the commutation relations of the Pauli spin matrices

$$[\sigma_x , \sigma_y] = i\sigma_z \text{ , etc.} \quad , \tag{6.10}$$

that

$$\frac{dr_1}{dt} = \omega_2 r_3 - \omega_3 r_2 \tag{6.11 a}$$

$$\frac{dr_2}{dt} = \omega_3 r_1 - \omega_1 r_3 \tag{6.11 b}$$

$$\frac{dr_3}{dt} = \omega_1 r_2 - \omega_2 r_1 \tag{6.11 c}$$

$$\frac{dr_4}{dt} = 0 \quad . \tag{6.12}$$

We now follow FVH and consider a linear vector space in which we have two vectors $\vec{r}$ and $\vec{\omega}$ that are defined by the components r_1 , r_2 , r_3 and ω_1 , ω_2 , ω_3 relative to three unit vectors $\vec{e}_1$, $\vec{e}_2$, $\vec{e}_3$. The equations (6.11) can then be written in the short-hand form

$$\frac{d\vec{r}}{dt} = \vec{\omega} \times \vec{r} \quad . \tag{6.13}$$

The vector $\vec{r}$ has a length $(r_1^2 + r_2^2 + r_3^2)^{\frac{1}{2}}$ which is equal to $r_4 = \overline{aa^* + bb^*} = 1$ and thus constant in time.

The beauty of this description is that the behaviour of the ensemble as described by the motion of vector $\vec{r}$ in the abstract $\vec{e}_1$, $\vec{e}_2$, $\vec{e}_3$ space is mathematically identical to the behaviour of a gyromagnet in a magnetic field in real space. So in order to see what happens one may use the language developed for discussing transient effects in magnetic resonance (see Abragam 1961, in particular Ch. II).

Of course we have to remember that the equations (6.5) and (6.13) as given, merely represent the time-dependent Schrödinger equation. In order to get the proper time evolution of the ensemble one should account for relaxation towards thermodynamic equilibrium. Later we shall follow the standard practice of adding phenomenological relaxation terms, but at the moment we neglect relaxation since it will prove relatively slow on the time scale of our experiment.

Let us first look at the physical meaning of the different components of the vector $\vec{r}$. The component r_3 is the analogue of the longitudinal magnetization in an NMR experiment and equal to the population difference of the two triplet levels T_z and T_y : $r_3 = \overline{aa^* - bb^*} = N_z - N_y$. The component r_2 is related to the expectation value of S_x and thus to the x-component of the magnetic dipole moment: $r_2 = i\,\overline{(ab^* - a^*b)} = - \langle \Psi | S_x | \Psi \rangle$. Finally the component r_1 appears to be related to a magnetic quadrupole moment; $r_1 = \overline{ab^* + a^*b} = - \langle \Psi | S_y S_z + S_z S_y | \Psi \rangle$.

The modulation of the phosphorescence is determined by the behaviour of r_3 , which measures the distribution of the systems over the radiative level T_z and the dark level T_y . In the absence of a microwave field ($V(t) = 0$) we have $\omega_1 = \omega_2 = 0$ and the vector $\vec{r}$ then precesses about $\vec{e}_3$ with angular velocity ω_0 ; as illustrated in

fig. 6.3 a the value of r_3 remains constant and so does the intensity of the phosphorescence. In order to see what happens when the perturbation V(t) is switched on it is advantageous to follow the practice customary in magnetic resonance of transforming to a primed frame rotating at the frequency ω about $\vec{e}_3$ in which the equation of motion becomes

$$\frac{\delta \vec{r}}{\delta t} = (\vec{\omega} - \omega \vec{e}_3') \times \vec{r} \quad . \tag{6.14}$$

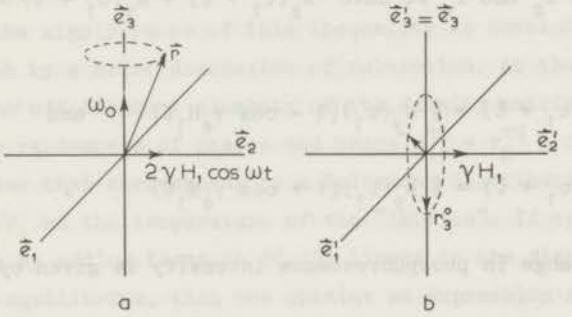

Fig. 6.3 a The vector space with $\vec{r}$ referred to the fixed axes $\vec{e}_1$, $\vec{e}_2$, $\vec{e}_3$.
Fig. 6.3 b The rotating vector space with unit vectors $\vec{e}_1'$, $\vec{e}_2'$, $\vec{e}_3'$ at exact resonance. The only component of $\vec{\omega}_{eff}$ is $\gamma_e H_1$ which is stationary along $\vec{e}_2'$. The vector $\vec{r}$ rotates about $\vec{e}_2'$ with angular frequency $\gamma_e H_1$; when r_3 points up along $\vec{e}_3'$ the entire population is in T_z; when it points down it is in T_y.

The linearly polarized field $\omega_2 = 2\gamma_e H_1 \cos \omega t$ is composed of a left and right rotating component. Only one has the proper sense of rotation and as usual in resonance phenomena we neglect the other (Abragam 1961, Ch. II). In the rotating frame the perturbation now appears stationary along the $\vec{e}_2'$ axis and the equation of motion (6.14) reduces to

$$\frac{\delta \vec{r}}{\delta t} = \{(\omega_0 - \omega)\,\vec{e}'_3 + \gamma_e H_1\,\vec{e}'_2\} \times \vec{r} = \vec{\omega}_{eff} \times \vec{r} \quad . \tag{6.15}$$

At exact resonance $\omega = \omega_0$ and the vector $\vec{r}$ precesses about the $\vec{e}'_2$ axis with angular frequency $\omega_1 = \gamma_e H_1$. If the component r_3 initially has a length $r_3(t_1) = r_3^o$ then on switching on the perturbation $V(t)$ at time $t = t_1$, the time dependence of r_3 will be given by $r_3(t_1 + \tilde{t}) = r_3^o \cos \gamma_e H_1 \tilde{t}$ (fig. 6.3 b).

In our experiment on the decay of quinoline at the moment we switch on the microwaves $r_3^o = N_z(t_1) - N_y(t_1) \approx - N_y(t_1)$. Because the duration of the microwave pulse is short as compared with the lifetimes of T_z and T_y we have $N_z(t_1 + \tilde{t}) + N_y(t_1 + \tilde{t}) = N_y(t_1)$ and thus

$$N_z(t_1 + \tilde{t}) = \tfrac{1}{2} N_y(t_1)(1 - \cos \gamma_e H_1 \tilde{t}) \quad \text{and} \tag{6.16}$$

$$N_y(t_1 + \tilde{t}) = \tfrac{1}{2} N_y(t_1)(1 + \cos \gamma_e H_1 \tilde{t}) \quad . \tag{6.17}$$

Hence the change in phosphorescence intensity is given by the expression

$$h_{y \to z}(t_1 + \tilde{t}) = \tfrac{1}{2} N_y(t_1)(1 - \cos \gamma_e H_1 \tilde{t})(k_z^r - k_y^r) \quad , \tag{6.18}$$

and this is borne out by the experiment. The maximum at $\tilde{t} = 0.27$ μs corresponds with $\gamma_e H_1 \tilde{t} = \pi$ and the minimum at $\tilde{t} = 0.54$ μs with $\gamma_e H_1 \tilde{t} = 2\pi$. When the pulse length is further increased the effect of a spread in resonance frequency between the individual systems comes into play and the phosphorescence signal tends to a value of about one half of the maximum at $\tilde{t} = 0.27$ μs .

In order to give a proper description of this effect we have to extend (6.13) with relaxation terms. Before doing so we first should mention a complicating factor that arises in our experiments. In the durene unit cell two sites occur, but from ESR experiments (Vincent and Maki 1965) it is known that four magnetically inequivalent quinoline molecules exist. Fortunately, there are only two different x-axes, which are almost perpendicular to each other and make an angle of about 5^o with the ab cleavage plane. In the experiment the

crystal was so oriented that the $\vec{H}_1$ field had to lie in this cleavage plane, with in general unequal field components along the x-axes of the different sites. By a subsequent rotation of $\vec{H}_1$ in the ab plane the curve of fig. 6.2 was obtained for which the 2π minimum proved deepest. On turning the crystal by a further 45° the minimum became much shallower and advanced to 0.43 μs. The curve in fig. 6.2 should correspond to a situation where $\vec{H}_1$ bisects the angle between the two x-axes and the effective field is about the same for all quinoline molecules. In this specific orientation the precession frequency $\gamma_e H_1/2\pi \simeq 2$ MHz a value which is seen to be larger than the linewidth of the Z - Y transition.

To show the significance of this inequality we conclude the present section by a brief discussion of relaxation. At thermodynamic equilibrium the off-diagonal elements of the density matrix vanish because of the randomness of phases and hence $r_1^{eq} = r_2^{eq} = 0$. Further, r_3^{eq} has a value that corresponds to a Boltzmann distribution over the levels T_y and T_z at the temperature of the "lattice". If we account for relaxation by adding terms to (6.13) linear in the displacement $\rho - \rho^{eq}$ from equilibrium, then one obtains an expression similar to the Bloch equations

$$\frac{d}{dt}\vec{r} = \vec{\omega} \times \vec{r} - \frac{r_1}{T_2'}\vec{e}_1 - \frac{r_2}{T_2'}\vec{e}_2 + \frac{(r_3^{eq} - r_3)}{T_1}\vec{e}_3 \quad . \tag{6.19}$$

In our experiment we expect $T_2' \simeq (2\pi\Delta\nu)^{-1}$ (Abragam and Bleany 1970, Ch. II), where $\Delta\nu$ is the linewidth of the zero-field transition. This relaxation time accounts for the disappearance of any non-zero value of r_1 and r_2 due to the spread in precessional velocities of the individual triplet systems. The relaxation time T_1 defines the rate with which r_3 approaches equilibrium. Since T_1 is of the order of seconds its effect can be neglected during the time interval of the microwave pulse. The coherence effects should occur when

$$|\gamma_e H_1| > 2\pi\Delta\nu \simeq \frac{1}{T_2'} \quad . \tag{6.20}$$

If this condition applies the time interval related to the angular frequency $\gamma_e H_1$ is smaller than the characteristic time T_2' with which

the individual triplet systems get out of phase. Hence, the coherent modulation is visible for times short as compared with T_2' ; it gradually decays due to the spread in effective field $\vec{\omega}_{eff}$ over the triplet systems. This spread in $\vec{\omega}_{eff}$ is caused by the inhomogeneity of $\vec{H}_1$ in amplitude and direction, the presence of four sites and the linewidth $\Delta\nu$. Since the decay of the modulation proceeds in a time of about $0.5 - 1$ μs we believe that it is mainly due to the spread in resonance frequency.

6.4 CONCLUSION

We have shown that the modulation of the phosphorescence that occurs when a strong microwave field is applied to a zero-field transition of a triplet state, may be explained conveniently by the FVH model. The analysis proceeds in the same way as the description of precessing magnetic moments in a magnetic field. However an important difference exists: in NMR and ESR there is a magnetic moment associated with each of the two states, while for a triplet state in zero-field $< S > = 0$ for all three spin states. What the two systems have in common is a matrix element of a dipole moment operator between the two states, which effects the coupling to the radiation field. In fact the only and necessary condition for the use of the FVH picture is that the matrix V(t) has the form

$$V(t) = \begin{pmatrix} 0 & V_{zy} \\ V_{yz} & 0 \end{pmatrix} . \qquad (6.21)$$

It may be worthwhile to mention that essentially the same model has been used to describe the phenomenon of photon echoes (Abella, Kurnit and Hartmann 1966). In their case an electric dipole moment operator connects the two states and again no expectation value of an electric or magnetic dipole moment is associated with the ground or excited state.

From the similarity of the behaviour of the triplet system with a

magnetic moment in a magnetic field one also understands the adiabatic inversion following a sweep through resonance. We expect that the necessary condition will be

$$\frac{1}{T_1} < \frac{1}{|\gamma_e H_1|} \left| \frac{d(\omega - \omega_0)}{dt} \right| < |\gamma_e H_1| \quad . \qquad (6.22)$$

A further condition for such an experiment is that the precessional frequency $\gamma_e H_1$ is at least in the order of magnitude of T_2^{-1}. Here T_2 now is a measure of the homogeneous spin-packet linewidth and accounts for the irreversible loss of coherence of the triplet systems (Abragam and Bleaney 1961, Ch. II). This condition is much easier to fulfil than (6.20), since in general T_2^{-1} is smaller than the value $(T_2')^{-1}$ that accounts for the total inhomogeneous linewidth of the spectrum.

The actual situation for an adiabatic passage may be rather complicated because in the zero-field spectra also forbidden transitions occur. For these transitions the matrix elements connecting the two states are smaller than $\gamma_e H_1$ and it may be impossible to fulfil condition (6.22). Accordingly, a mixture of saturation and inversion may result.

From the FVH model together with the present results one would expect spin-echo experiments to be feasible. The description again is similar to the well-known picture for NMR. By a $\frac{\pi}{2}$ pulse a vector $\vec{r}=r_3^o\vec{e}_3$ is first brought along the $\vec{e}_1'$ axis (fig. 6.3 b) and subsequently it fades out because of the spread in resonance frequencies of the individual spins. A second 180° pulse inverts the phase differences and an echo should be formed along the $\vec{e}_1'$ axis. Since $r_2 = - < S_x >$ the echo must manifest itself as a pulse of microwave power spontaneously emitted by the triplet spin system.

An important result from such an experiment would be the "genuine" relaxation time T_2 associated with the irreversible loss in coherence between the triplet spin systems. This relaxation time T_2 has never been measured for phosphorescent triplet states but even for electron paramagnetic systems in general only a few experimental results are available. The reason for this scarcity of information

about T_2 in electron paramagnetic systems as opposed to nuclear magnetic systems is the experimental problems that arise in fulfilling the condition equivalent to (6.20).

An important advantage of doing spin-echo experiments in zero-field resides in the following. As we have seen, the resonance transitions in zero-field tend to be far narrower than in normal ESR experiments because h.f. interaction becomes a second order effect in the absence of an external field. As a result the condition (6.20) can be fulfilled without having to face the serious experimental problems associated with strong microwave fields of very short duration (Mims 1965, Rowan 1965, Brandle et al. 1970). We think that the electron spin-echo technique in zero-field is promising and may provide valuable information about the interactions responsible for relaxation processes.

A P P E N D I X

PREPARATION OF THE CRYSTALS

The crystals of quinoxaline-h_6 and quinoxaline-d_6 in durene were kindly supplied by the Koninklijke/Shell-Laboratorium, Amsterdam and their preparation described by de Groot et al. (1968), will be repeated here. Quinoxaline-h_6 was prepared from a commercial sample (Schuchardt) by vacuum distillation and subsequent multiple zone refining in a nitrogen atmosphere. Quinoxaline-d_6 was synthesized by Mr. M.J. van den Brink of KSLA by contacting quinoxaline-h_6 with a large excess of 0.8% DCl in D_2O for 60 hours at 230°C in the presence of a Pt-catalyst. The product was isolated from the reaction mixture by extraction and then purified by vacuum distillation and chromatography over Al_2O_3. The sample of quinoxaline-d_6 thus obtained had a d/h ratio of 96.4% and the the total mass spectrometric analysis showed that it consisted of 80.2% quinoxaline-d_6 , 17.9% quinoxaline-d_5-h_1 and 1.9% quinoxaline-d_4-h_2.

Durene (Shell Chemical Corporation) was sublimed under vacuum and then submitted to multiple zone refining. Two single crystals, one doped with quinoxaline-h_6 and the other with quinoxaline-d_6 were grown by slowly passing a sealed tube containing a 1% solution of quinoxaline in durene under nitrogen through a sharp temperature gradient. In the case of quinoxaline-d_6 an average concentration of 0.014% was found in the crystal.

The samples of quinoline-h_7 and quinoline-d_7 in durene were kindly prepared by Mrs. G.M. Gorter-la Roij, Mr. J. van Egmond and Mr. M. Noort. Quinoline-h_7 was prepared from a commercial sample (Fluka) by vacuum distillation. Quinoline-d_7 was synthesized from quinoline-h_7 in the same way as quinoxaline-d_6 , except for a 150 hours contact time with the DCl-D_2O mixture at 180-190°C and purification by vacuum distillation only. The sample of quinoline-d_7 had a d/h ratio of 96.8% and the total mass spectrometric analysis showed that it consisted of 78.8% of quinoline-d_7 , 19.2% quinoline-d_6-h_1 , 2.1% quinoline-d_5-h_2 . Durene (Baker) was also vacuum sublimed and then

submitted to multiple zone refining. The mixed crystals of quinoline-h_7 and -d_7 in durene were grown in a similar way as described above; the starting solution containing 3% of the guest. The concentration in the resulting mixed crystals was not determined.

The single crystal of naphthalene-d_8 in durene was made by Mr. M. Noort. Naphthalene-d_8 was kindly supplied by the Koninklijke/ Shell-Laboratorium, Amsterdam. The sample showed a d/h ratio of 97.8% and contained 83.6% naphthalene-d_8, 15.1% naphthalene-d_7-h_1 and 1.2% naphthalene-d_6-h_2. Durene (Baker) was purified by multiple zone refining and then chromatographed over a column of Al_2O_3. The mixed crystal was grown from a 3% solution of naphthalene-d_8 in durene. The concentration of naphthalene-d_8 in the mixed crystal was not determined.

REFERENCES

Abella, I.D., Kurnit, N.A. and Hartmann, S.R., 1966, Phys.Rev. 141,391.

Abragam, A., 1961, The principles of nuclear magnetism, Oxford, Clarendon Press.

Abragam, A. and Bleaney, B., 1970, Electron paramagnetic resonance of transition ions, Oxford, Clarendon Press.

Antheunis, D.A., Schmidt, J. and van der Waals, J.H., 1970, Chem.Phys. Letters 6, 255.

Brandle, R., Krüger, G.J. and Müller-Warmuth, W., 1970, Z.für Naturf. 25a, 1.

Brossel, J. and Kastler, A., 1949, Comptes Rendus 229, 1213.

Brossel, J. and Bitter, F., 1952, Phys.Rev. 86, 308.

Buckley, M.J. and Harris, C.B., 1970, Chem.Phys. Letters 5, 205.

Burland, D.M., 1971, to be published.

Chan, Iu-Yam, Schmidt, J. and van der Waals, J.H., 1969, Chem.Phys. Letters 5, 269.

Chaudhuri, N.K. and El-Sayed, M.A., 1966, J.Chem.Phys. 44, 3728.

El-Sayed, M.A., Owens, D.V. and Tinti, D.S., 1970, Chem.Phys. Letters 6, 395.

Erickson, L.E., 1966, Phys.Rev. 143, 295.

Fayer, M.D., Harris, C.B. and Yuen, D.A., 1970, J.Chem.Phys. 53, 4719.

Feynman, R.P., Vernon, F.L. and Hellwarth, R.W., 1957, J.Appl.Phys. 28, 49.

Geschwind, S., Collins, R.J. and Schawlow, A.L., 1959, Phys.Rev. Letters 3, 544.

de Groot, M.S., Hesselmann, I.A.M. and van der Waals, J.H., 1967, Mol.Phys. 12, 259.

de Groot, M.S., Hesselmann, I.A.M., Schmidt, J. and van der Waals, J.H., 1968, Mol.Phys. 15, 17.

Guibé, L., 1962, Ann.Phys. 7, 177.

Hammer, A., Schwoerer, M. and Sixl, H., 1970, Chem.Phys. Letters 7, 434.

Harris, C.B., Tinti, D.S., El-Sayed, M.A. and Maki, A.H., 1969, Chem.Phys. Letters 4, 409.

Harris, C.B., 1971, J.Chem.Phys. 54, 972.

Hirota, N., Hutchison, C.A. and Palmer, P., 1964, J.Chem.Phys. 40, 3717.

Hornig, A.W. and Hyde, J.S., 1963, Mol.Phys. 6, 34.

Hutchison, C.A. and Mangum, B.W., 1958, J.Chem.Phys. 29, 952.

Hutchison, C.A. and Mangum, B.W., 1960, J.Chem.Phys. 32, 1261.

Hutchison, C.A. and Mangum, B.W., 1961, J.Chem.Phys. 34, 908.

Hutchison, C.A., 1967, The Triplet State, Cambridge University Press, 63.

Hutchison, C.A., Nicholas, J.V. and Scott, G.W., 1970, J.Chem.Phys. 53, 1906.

Jablonski, A., 1933, Nature 131, 839.

Jen, C.K., Aamodt, L.C. and Piksis, A.H. 1967, The Triplet State, Cambridge University Press, 143.

Kwiram, A.L., 1967, Chem.Phys. Letters 1, 272.

Lewis, G.N. and Kasha, M., 1944, J.Am.Chem.Soc. 66, 2100.

Lewis, G.N. and Kasha, M., 1945, J.Am.Chem.Soc. 67, 994.

Lucken, E.A.C., 1961, Trans.Faraday Soc. 57,799.

Mims, W.B., 1965, Rev.Sc.Instr. 36, 1472.

Moreno, T., 1948, Microwave transmission design date, McGraw Hill, New York.

Pierce, J.R., Traveling Wave Tubes, O. vah Nostrand Co. Inc., Princeton, New Jersey.

Robertson, J.M., 1933, Proc.Roy.Soc. (London) A 141, 594; ibid. A 142, 659.

Robinson, G.W. and Frosch, R.P. 1963, J.Chem.Phys. 38, 1187.

Rowan, L.G., Hahn, E.L. and Mims, W.B., 1965, Phys.Rev. 137, A 61.

Schempp, E. and Bray, P.J., 1967, J.Chem.Phys. 46, 1186.

Schmidt, J., Hesselmann, I.A.M., de Groot, M.S. and van der Waals, J.H., 1967, Chem.Phys. Letters 1, 434.

Schmidt, J. and van der Waals, J.H., 1968, Chem.Phys. Letters 2, 640.

Schmidt, J. and van der Waals, J.H., 1969, Chem.Phys. Letters 3, 546.

Schmidt, J., Veeman, W.S. and van der Waals, J.H., 1969, Chem.Phys. Letters 4, 341.

Schmidt, J., Chan, Iu-Yam and van der Waals, J.H., 1970, 20^{e} Réunion de la Société de Chimie Physique, Paris, J.Chim.Phys. 1970, 116.

Schwoerer, M. and Sixl, H., 1968, Chem.Phys. Letters 2, 14.

Schwoerer, M. and Sixl, H., 1969, Z.für Naturf. 24a, 952.

Sharnoff, M., 1967, J.Chem.Phys. 46, 3263.

Sixl, H. and Schwoerer, M.,1970, Chem.Phys. Letters 6, 21.

Tinti, D.S., El-Sayed, M.A., Maki, A.H. and Harris, C.B., 1969, Chem.Phys. Letters 3, 343.

Vincent, J.S. and Maki, A.H., 1963, J.Chem.Phys. 39, 3088.

Vincent, J.S. and Maki, A.H., 1965, J.Chem.Phys. 42, 865.

Vincent, J.S., 1970, J.Chem.Phys. 52, 3714.

van Vleck, J.H., 1951, Rev.Mod.Phys. 23, 213.

van der Waals, J.H. and de Groot, M.S., 1959, Mol.Phys. 2, 333.

van der Waals, J.H. and de Groot, M.S., 1967, The Triplet State, Cambridge University Press, 101.

Watkins, D.A., 1958, Topics in Electromagnetic Theory, John Wiley and Sons, Inc., New York.

Webb, R.H., 1962, Rev.Sc.Instr. 33, 732.

Ziegler, S.M. and El-Sayed, M.A., 1970, J.Chem.Phys. 52, 3257.

SUMMARY

In the first chapter of this thesis it is shown that microwaves may affect the phosphorescence of organic molecules. The effect is observed at liquid helium temperatures, on molecules diluted in a crystalline matrix and excited by u.v. irradiation into their lowest (phosphorescent) triplet state. The experiments are based on the idea that radio frequency transitions, induced between the spin components of the triplet state, show up as a change in intensity of the phosphorescence. Although resembling the well known experiments of Brossel and Kastler on Hg atoms and of Geschwind, Collins and Schawlow on Cr^{3+} ions in Al_2O_3 , some important differences exist. The experiments are done in the absence of an external magnetic field and further the polarizations of the radio frequency transitions are determined by the molecule.

The purpose of this thesis is to show the possibilities of this new technique for the study of the magnetic and optical properties of the triplet state. To this end we discuss three kinds of experiments and illustrate them with results on three related molecules: naphthalene and the aza-naphthalenes quinoline and quinoxaline.

Steady state experiments. The system is irradiated continuously with u.v. light in the presence of the microwave field that is swept slowly through one of the resonant transitions. In this way one obtains the line shape of the transition. The typical structures that appear in the spectra of the aza-naphthalenes are explained by hyperfine and quadrupole interaction involving the nitrogen nuclei. From these structures one finds the quadrupole splitting of the nitrogen nuclei in the excited triplet state.

Transient experiments. The system is irradiated during a limited period with u.v. light at a temperature where the relaxation between the spin components is negligible. Spectacular changes in the phosphorescence intensity may then be produced by sweeping the microwave field suddenly through resonance during the decay of the system after switching off the exciting light. With this kind of experiments one solves the dynamics of populating and depopulating the individual spin levels of the triplet state. The results provide information about processes involving spin-orbit coupling and radiationless transitions in these polyatomic molecules.

Coherence experiments. The triplet system is subjected to a strong monochromatic microwave field resonant with one of the zero-field transitions and with an amplitude exceeding the linewidth of the zero-field transition. In this situation the electron spins are coupled coherently to the driving microwave field. One observes a modulation of the phosphorescence with a frequency determined by the amplitude of the field. With the help of an elegant model developed by Feynman, Vernon and Hellwarth, it is possible to describe the coherent coupling in a way analogous to the behaviour of a gyromagnet in a magnetic field. From such coherence experiments we hope to obtain detailed information about relaxation processes in phosphorescent triplet states.

SAMENVATTING

In het begin van dit proefschrift wordt aangetoond hoe men met microgolven de fosforescentie kan beïnvloeden van organische moleculen die door bestraling met ultra violet licht zijn geexciteerd in de laagste (fosforescerende) triplet toestand. Deze moleculen zijn verdund aanwezig in een kristallijne matrix en het verschijnsel nemen we waar bij de temperatuur van vloeibaar helium. De experimenten berusten op het idee dat radio-frequente overgangen, geïnduceerd tussen de spin componenten van de triplet toestand, zich uiten via een intensiteitsverandering van de fosforescentie. Hoewel er punten van overeenkomst zijn met de bekende experimenten van Brossel en Kastler aan Hg atomen en Geschwind, Collins en Schawlow aan Cr^{3+} ionen in Al_2O_3, zijn er enkele essentiele verschillen. In de eerste plaats is er geen uitwendig magneetveld aanwezig en verder zijn de radio-frequente overgangen lineair gepolariseerd volgens richtingen vastgelegd door het molecuul.

Het doel van dit proefschrift is om de mogelijkheden aan te tonen die deze nieuwe techniek biedt voor de studie van de magnetische en optische eigenschappen van de triplet toestand. Daartoe behandelen we drie soorten experimenten en illustreren ze met resultaten aan drie verwante moleculen: naftaleen en de aza-naftalenen, chinoline en chinoxaline.

Ten eerste "steady state" experimenten, waarin men het systeem continu bestraalt met u.v. licht in de aanwezigheid van het microgolfveld dat langzaam in frequentie wordt gevarieerd. Op deze manier verkrijgt men de lijnvorm van de overgangen. De typische structuur die blijkt op te treden in de spectra van de aza-naftalenen kunnen we ver-

klaren door middel van de hyperfijn- en quadrupoolinteractie van de stikstofkernen. Uit deze structuur is het dan mogelijk de quadrupoolsplitsing van de stikstofkernen in de triplet toestand te berekenen.

Ten tweede "transient" experimenten waarin men het systeem gedurende een beperkte periode met u.v. licht exciteert bij een temperatuur, waar de relaxatie tussen de spin componenten verwaarloosbaar is. Na het uitzetten van het exciterende licht laat men gedurende het verval van de fosforescentie het microgolfveld plotseling een snelle passage door resonantie maken. Op deze wijze induceert men aanzienlijke veranderingen in de intensiteit van de fosforescentie. Met behulp van dit soort experimenten kan men de dynamiek van het bevolken en ontvolken van de individuele niveaus van de triplet toestand oplossen. De resultaten verschaffen informatie over spin-baan koppeling en stralingsloze processen in dit soort veelatomige moleculen.

Ten derde coherentie experimenten. Men onderwerpt het triplet systeem aan een sterk monochromatisch microgolfveld, resonant met één van de overgangen en met een amplitude groter dan de lijnbreedte. Er treedt dan een coherente koppeling op van het triplet systeem aan het microgolfveld. Als gevolg neemt men een modulatie waar van de fosforescentie met een frequentie die wordt bepaald door de amplitude van het veld. Met behulp van een elegant model, gegeven door Feynman, Vernon en Hellwarth, is het mogelijk de coherentie te beschrijven op een manier analoog aan het gedrag van een gyromagneet in een magneetveld. Met dit soort coherentie experimenten hopen we in de toekomst gedetailleerde informatie te verkrijgen over de relaxatie processen in de fosforescerende triplet toestand.

Op verzoek van de Faculteit der Wiskunde en Natuurwetenschappen volgt hier een kort overzicht van mijn studie.

Nadat ik in 1954 het diploma HBS-B heb gehaald aan de toenmalige 3e-vijfjarige HBS-B te Amsterdam, ben ik mijn studie begonnen aan de Universiteit van Amsterdam. Na mijn candidaatsexamen d in 1958 vingen mijn werkzaamheden aan in de afdeling microgolf spectroscopie van het Zeeman Laboratorium. Deze afdeling werd in 1960 toegevoegd aan het Natuurkundig Laboratorium, waardoor de leiding in handen kwam van Prof.Dr. G.W. Rathenau. De experimenten waarbij ik toen heb geassisteerd varieerden van microgolf spectroscopie aan gassen tot ferromagnetische resonantie in dunne metaalfilms. In 1961 werd het doctoraalexamen in de experimentele natuurkunde afgelegd.

Ingelijfd bij de Koninklijke Landmacht bracht ik een belangrijk deel van mijn dienstplicht door op het Physisch Laboratorium van RVO-TNO.

In 1963 trad ik in dienst van het Koninklijke/Shell-Laboratorium, Amsterdam. In de afdeling Fundamentele Research heb ik onder andere meegewerkt aan kernspin resonantie proeven in vloeistoffen.

In 1964 stelde het Koninklijke/Shell-Laboratorium, Amsterdam mij in staat te studeren aan de Ecole Polytechnique te Parijs. Hier heb ik onder de voortvarende leiding gestaan van Professor I. Solomon. Tijdens mijn verblijf aldaar werd aan een verscheidenheid van experimenten gewerkt: kernspin relaxatie in vaste stoffen, thermische detectie van ESR en ESR in halfgeleiders.

In 1966 ben ik teruggekeerd naar het Koninklijke/Shell-Laboratorium, Amsterdam waar werd begonnen met het opbouwen van een ENDOR opstelling.

In 1968 ben ik als wetenschappelijk medewerker in dienst getreden van de Rijksuniversiteit te Leiden en vingen mijn werkzaamheden aan op het Kamerlingh Onnes Laboratorium in de werkgroep Moleculen in Aangeslagen Toestand onder leiding van Prof.Dr. J.H. van der Waals.

De oplettende lezer heeft gemerkt dat op de titelpagina van dit proefschrift de suggestie wordt gewekt als zou de inhoud het resultaat zijn van de inspanning van één enkel persoon. Dit idee echter berust op een misvatting. In werkelijkheid is deze dissertatie de vrucht van een samenwerking in de werkgroep Moleculen in Aangeslagen Toestand. De dagelijkse discussies met de andere leden van deze werkgroep en de internationale contacten via congressen of bezoekers hebben de basis gelegd voor de ideeën waarvan de concrete resultaten zijn beschreven in de voorgaande paginas.

Al deze ideeën waren ideeën gebleven als ik geen hulp had gekregen om de experimenten uit te voeren. Zo zijn de kristallen waaraan de metingen zijn gedaan enerzijds ter beschikking gesteld door het Koninklijke/Shell-Laboratorium, Amsterdam, en anderzijds geprepareerd door mevrouw G.M. Gorter-la Roij en de heren M. Noort en Drs. J. van Egmond. Verder ben ik op het Kamerlingh Onnes Laboratorium omringd geweest met technische faciliteiten waarvoor een groot aantal personen zorg dragen. Hiervan wil ik in het bijzonder noemen de heren T. Nieboer, J.F. Benning, J. van den Berg en L. van As. Voor de illustratie van de resultaten heb ik nooit tevergeefs een beroep hoeven doen op de heer W.F. Tegelaar en in het bijzonder voor dit proefschrift op de heer H.J. Rijskamp. Tenslotte heeft Marian Zurburg zich belast met het typen van het manuscript zonder ooit haar goede humeur erbij te verliezen.